COLLEGE OF SOCIAL SCIENCE

DEPARTMENT OF GEOGRAPHY AND ENVIRONMENTAL STUDIES

M.A RESEARCH THESIS ON:

ANALYSIS OF LAND USE/COVER CHANGE AND ITS CORRELATION WITH LAND SURFACE TEMPERATURE IN ASELLA AND ITS SURROUNDING AREA, ETHIOPIA

A Thesis Submitted to the Department of Geography and Environmental Studies in Partial Fulfilment of the Requirements for the Degree of Master of Arts in Geography and Environmental Studies (Specialization in GIS, Remote Sensing, and Digital Cartography)

BY: DAWIT DESALEGN TOLA

(GSR/4520/15)

ADVISOR

MULUNEH W/TSADIK (PhD)

Addis Ababa, Ethiopia

June, 2024

ADDIS ABABA UNIVERSITY

COLLEGE OF SOCIAL SCIENCE

This is to certify that the thesis prepared by: Dawit Desalegn Tola, entitled: **ANALYSIS OF LAND USE/COVER CHANGE AND ITS CORRELATION WITH LAND SURFACE TEMPERATURE IN ASELLA AND ITS SURROUNDING AREA**. and submitted in partial fulfillment of the requirement for the degree of Master of Arts in Geography and Environmental Studies (GIS, Remote Sensing, and Digital Cartography), This conforms to the university's rules and fulfills the recognized requirements for originality and quality.

Approved by the Examining Committee:

Advisor	Signature	Date
Internal Examiner	Signature	Date
External Examiner	Signature	Date
College or center of Chairperson	Signature	Date

Ackacknowledgments

Above all, I would like to convey my appreciation to the almighty God for making it possible and giving me the perseverance and fortitude I needed to finish my studies in the allotted short time. next to God, I want to express my sincere gratitude and debt of gratitude to my advisor, Dr. Muluneh W/tsadik, for helping me with this study from the very beginning to the end, for sharing their time with me for insightful conversations and for providing me with kind, useful advice.

Furthermore, I would like to thank the entire Geography department team and the GIS, Remote sensing, and Digital cartography stream staff members for providing access to the lab—facility and for unreserved support.

For providing me with the data and information I required to finish this work, the Ethiopian Meteorology Agency, Central Statistical Agency, and Ethiopian Space Science and Geospatial Institute have my sincere gratitude.

I especially want to thank my classmates and family for their support and gratitude over the years. In closing, I want to thank everyone who has ever been my friend, teacher, or supporter as I started this arduous road. Their surnames are also too many to mention, but many of them motivated me to advance and study.

Contents

List of Tables

List of Figures

Appendices

Acronyms and Abbreviations

CSA	Central Statistic Agency
DEM	Digital Elevation Model
DN	Digital Number
ERDAS	Earth Resources Data Analysis System
GIS	Geographical Information System
IDW	Inverse Distance Weighted
LSE	Land Surface Emissivity
LST	Land Surface Temperature
LU/CC	Land Use/Cover Change
LU/LC	Land Use/Land cover
NDVI	Normalized Difference Vegetation Index
NIR	Near Infrared Radiation
OLI	Operational Land Imager
RS	Remote Sensing
SST	Increased Sea Surface Temperature
SSGI	Space Science and Geospatial Institute
TM	Thematic Mapper
TIRS	Thermal Infrared Sensor
TOA	Top of Atmospheric
UHI	Urban Heat Island
USGS	United States Geological Survey
UTM	Universal Transverse Mercator
WGS	World Geodetic Systeam

Abstract

One of the primary environmental issues and challenges that have a significant impact on the growth of agriculture and urban areas is the change in land use and cover change (LU/LC). The world is currently dealing with an excessive rise in land surface temperature (LST) year to year. The present study has investigated the analysis of land use/cover change and its correlation with land surface temperature. The study was carried out in Asella and its surrounding area, located in the Oromia region, Eastern Ethiopia. LU/CC, NDVI, and LST were extracted from Landsat TM (1987), Landsat ETM + (2005), and Landsat 8 OLI/TIRS (2023) using GIS and remote sensing tools. A split window algorithm was used to calculate the land surface temperature. Using geospatial techniques, changes in LU/LC that took place throughout the research area between 1987 and 2023 were assessed, examined, and validated by Google Earth. The result of LU/CC showed that farmland land covered more than 53% throughout the study times (1987–2023) Based on the analysis, the majority of regions with lower LST in 1987 and higher LST in 2023. This occurred due to an increase in various LU/LC changes, particularly the study area's declining plant cover. Through the use of zonal statistics as a table to link the LST and the LU/LC class parameters, it has been discovered that a negative association between LST and vegetation cover. The findings for land surface temperature indicated that the values ranged from 8.74ºC to 48.85ºC in the Southwestern, Ziway wetter bodies, and Southeastern along Chilalo Terara. The high NDVI number is what caused this to occur. In contrast, the LST values in the central, northeastern, northern, and west regions were high, reaching as high as 48.85ºC. Consequently, a visual comparison of 1987, 2005, and 2023 images demonstrated the significant influence that LU/LC type and NDVI status have on the variability of LST values. Reversing the LU/CC has proven to be challenging. Nonetheless, several actions need to be taken by environmental specialists and pertinent organizations to reduce their influence on the environment and LST. The efficiency of employing geospatial tools as time- and money-saving techniques for LST analysis and evaluation is demonstrated by this study.

Keywords: Remote sensing, GIS, LU/LC, LU/CC, LST, NDVI, and Landsat image

CHAPTER ONE

INTRODUCTION

1.1.Background

Earth has experienced ongoing transformations over long periods, and one significant contemporary challenge is the growing rise in land surface temperature (LST) observed year after year. These temperature rises have significant effects on the earth's systems and human societies. Among the drivers of these changes, land use/cover changes (LU/CC) alterations, stemming from both natural and human-induced processes, have emerged as key contributors to global and regional climate patterns (Ramachandra, 2021). In recent times, the earth has been changing much. The major problem we face is the increase in heat on the land surface. Worldwide, changes in land use/land cover (LU/LC) lead to environmental shifts, fluctuations in rainy seasons, rising sea levels, and increasing LST. Massive LU/CC results from the need for land for settlement and agriculture due to the growing human population (Mohanrajan & Loganathan, 2020). Land use should align with land capacity and respect the overall climate conditions and environment (Thornton, & Herrero, 2010). The increasing LST from converting vegetative surfaces into artificial habitats is a significant environmental concern in rural and urban areas. Monitoring this phenomenon involves assessing crucial data using thermal bands from various sensors, focusing specifically on LST (Tafesse, & Suryabhagavan, 2019). Natural processes such as wildfires, volcanic eruptions, tectonic movements, and human activities like urbanization, deforestation, agriculture expansion, and industrialization have severely changed the earth's surface. LU/CC can worsen climate change by increasing greenhouse gases and creating heat islands with higher temperatures, which amplify local and global warming through feedback loops (Gemeda et al., 2023). Moreover, LU/LC modifications may trigger feedback loops that intensify global warming. Deforestation, for example, diminishes the area of forests, which are important carbon sinks. As a result, there is an increase in atmospheric levels of carbon dioxide and warming.

Due to significant changes in LU/LC, global warming is getting worse. The land is the primary natural resource humans use for infrastructure, social, economic, and other purposes. It is the supplier of the supplies required for these tasks. Land usage has changed throughout history, is still changing now, and will probably keep changing in the future (Seyam et al., 2023). Therefore, to lessen the negative consequences of global warming on changes in land use and cover, it is

imperative that these issues be addressed, and sustainable land management techniques be put into place. According to Solaimani et al., (2010), significant LU/CC occurs in many different parts of the world due to varying environmental conditions.

LU/CC can seriously impact future food security and environmental quality, affecting human well-being and the goals of land management systems (Wheeler & Von Braun, 2013). Therefore impacts environmental quality, land administration goals, and human well-being. Consequently, LU/CC is a critical issue for sustainable development and a dynamic field of study. The complex interactions between various biophysical and socioeconomic factors at different temporal and spatial scales drive LU/LC dynamics. (Reid et al., 2000).

One of the primary causes of global warming in Africa is the significant changes in LU/LC. These LU/LC changes lead to environmental alterations, variations in rainy seasons, and fluctuations in LST (Kundu & Pandey, 2020). Developing countries have played an important role in high growth rates of urbanization. The most significant contributors to the observed changes in urban surface temperature and its surrounding areas in recent years (Ayanlade et al., 2021). Understanding the spatial distribution and temporal trends of land surface temperature in urban environments is important for managing sustainable urbanization (Zhang et al., 2022). Urbanization changes land use patterns and LST. Africa's rapidly expanding cities are expected to significantly increase their urban population by 2050, highlighting the need for sustainable urban development to manage these changes effectively (Kassouri & Adewole, 2022). Ethiopia's rapid urban population growth, with its urban population nearly quadrupling from 15.2 million in 2012 to 42.3 million in 2037, growing at an annual rate of 3.8%, highlights the significant impact of LU/LC changes on LST (Alliance, 2015). Urban growth and its surrounding areas, including population increase, infrastructure development, and changes in land use such as the expansion of commercial and residential areas, significantly impact LST (Chen et al., 2017).

LST is a critical parameter for both local and global surface energies, and water bodies, and provides useful information about surface properties and conditions. Determining the spatial distribution of LST patterns is also helpful in comprehending several problems, including evapotranspiration, temperature change, and urban environmental conditions (Govind & Ramesh, 2019). Urban heat islands, drought, public health, and climate change are all correlated with LST. It is important for comprehending and tackling a range of societal and environmental issues (Mo

et al., 2021). According to (Rajeshwari & Mani, 2014), LST is the temperature emitted by the earth's surface, expressed in Kelvin. It represents the perceived temperature of the land, influenced by the amount of solar radiation absorbed by the surface (Kumar and Singh, 2016), as derived from direct measurements/ from remotely sensed information.

The investigation of LU/CC and LST impacts is now more valuable for advanced environmental management because of remote sensing sensors (Sresto et al., 2022). Using RS and GIS has shown to be especially crucial for assessing and analyzing LU/CC and LST variations (Attri et al., 2015). Therefore, the present research has made an effort to assess the correlations between LU/CC, NDVI, and land surface temperature (LST) in Asella town and its surrounding areas using GIS and RS. This approach enhances understanding of LU/LC impacts on LST, aiding informed decisions in environmental preservation and land management.

1.2 Statement of the problem

Nowadays, global warming is a pressing issue caused by massive LU/CC (Ramankutty, N. et al,2006). LST can be defined as the temperature felt when the land surface is touched. It is essential for determining the temperature of the land and is important for tracking changes in the environment. For millions of people, forests provide their main income source and underpin numerous nations' economies. Because vegetation stores and takes in carbon dioxide from the environment, it slows down the rate of climate change. Due to increased human and cattle populations, pervasive rural poverty, and other factors, forest resources worldwide are under tremendous strain, leading to deforestation and degradation despite their critical relevance in regulating climate and providing subsistence (*F*AO, 2011).

Urban and rural areas are significantly challenged by the accelerated rate of global warming (Grimmond et al., 2007). LU/CC patterns have shifted markedly due to population growth, industrialization, and various human and natural processes. These modifications are a primary driver behind the increase in LST. Environmental challenges and global warming are pressing global issues affecting both industrialized and developing countries alike. Climate change results from unsustainable practices such as overgrazing, deforestation, unplanned settlement development, etc. These temperature fluctuations primarily stem from LU/CC, impacting LST and local climate dynamics (Gupta et al., 2020). Human activities such as industrialization, agricultural development, and urbanization continuously reshape landscapes, leading to unprecedented

variations in temperature regimes (Ellis, 2021). Research indicates that LU/CC, including overgrazing, deforestation, and unregulated settlement, contribute to rising LST levels, exacerbating socioeconomic vulnerability and environmental degradation.

Due to human forces, Asella and its surrounding areas' land use patterns and land cover types have occasionally changed. The beauty of the environment, energy efficiency, human health, and living standards in metropolitan areas may suffer due to these changes. Solar radiation absorption and thermal conductivity increased due to LU/CC, notably the fast expansion of uncontrolled agricultural land and urban areas at the cost of other land uses, including grasslands, woodlands, and shrublands. The loss of forests causes several ecological, social, and economic problems, such as the extinction of biotic groups, decreased biodiversity, soil erosion, local warming, and income loss for forest inhabitants.

Despite recognizing the importance of understanding the correlation between LU/CC and LST dynamics, there remains a research gap in comprehensively assessing this relationship in specific areas like Asella and its surrounding area, in the Oromia region of Ethiopia. Existing studies on LU/CC and LST dynamics in Asella and its surrounding areas are lacking. This study addresses these gaps by analyzing LU/LC changes and their correlation with LST in Asella and its surrounding areas from 1987 to 2023, providing localized insights to support evidence-based decision-making and sustainable land use planning. The region's diverse vegetation, variable climate patterns, distinct topographic features, and substantial LU/LC changes make it an ideal subject for this research. Utilizing advanced remote sensing techniques, robust conceptual frameworks, and GIS technologies, this study provides localized insights into the drivers and implications of LU/CC shifts on LST dynamics. This Master's thesis is unique in its approach, addressing an unexplored topic in this study area and aiding in the establishment of climate adaptation plans and sustainable land management practices.

1.3 Objectives

1.3.1 General objective

The general objectives of this research focus on the analysis of LU/CC and its correlation with LST using Landsat imagery and geospatial techniques.

1.3.2 Specific objectives

The following three Specific goals were developed to fulfill the overall objective:

1. To assess LU/LC change in the period between 1987 and 2023 in the study area.
2. To assess the LST Variations between 1987 to 2023.
3. To analyze the temporal and spatial changes in LST about LU/LC dynamics in the study area.

1.4. Research questions

Knowing the influence of LU/CC and vegetation on LST serves to be useful for land management and land use planning strategies focused on LST mitigation and adaptation of the research area to the challenges of climate change. Moreover, it responds to the subsequent research inquiries::

- What are the major LU/LC classes in the study area?
- What are the temporal trends and spatial patterns of land surface temperature in the study area during this period?
- What is the correlation between LU/LC, LST, and NDVI in the study area?

1.5. Significance of the study

Asella and its surrounding areas were characterized by diverse landscapes, including built-up areas, dry soil, rocks, concrete infrastructure, water bodies, wetlands, forests, grasslands, shrublands, and farmland. Although the impact of these landscapes on LST varies, built-up areas and concrete infrastructure typically result in higher LST. On the other hand, they have cultivated land, marshes, forests, and bodies of water generally lower LST. The significance of the study lies in its ability to provide essential information about LU/LC patterns and variations in LST in the Asella and its surrounding areas. It is, first and foremost, a priceless resource for environmental experts, managers of natural resources, policymakers, and other authorities tasked with overseeing land management in both urban and rural areas. Decision-makers can create knowledgeable rules and guidelines to reduce negative effects on the environment and nearby communities by receiving specific insights on how LU/CC and LST change over time. Furthermore, the study's conclusions can be used as a guide for the next studies, offering a strong basis for more research into the intricate connection between LST and LU/LC dynamics.

1.6. Study's scope

The study focuses on Asella and its surrounding areas in Oromia, Ethiopia, selected for their diverse LU/LC patterns and their relevance to the research objectives. The region has experienced significant LU/CC changes, contributing to periodic increases in LST. Local perceptions indicate rising LST, prompting this study to provide empirical evidence through detailed analysis. Different land use categories, including urban regions, woods, agricultural lands, aquatic bodies, and barren ground, are methodically analyzed. Data is being gathered and analyzed using GIS methods and remote sensing imagery to identify patterns of change over time. To verify the LU/CC's classification accuracy and LST extraction techniques and guarantee the dependability of the results, field verification, and Google Earth verification are also being carried out. Additionally, this study examines how LST and LU/CC dynamics impact water resource management, agricultural land, and settlements in Asella and its surrounding areas. By providing evidence-based insights, it aims to guide sustainable land management practices and develop strategies to mitigate environmental degradation and adapt to the region's changing climate.

1.7. Limitations of the study

Every effort was made to gather the necessary primary and secondary data for the study, together with precise procedural analysis and technical interpretations.

Nevertheless, this study has the following limitations:

- Difficulty in obtaining information from different organizations while maintaining the normal process.
- When downloading images the connection of the internet problem.

I solved the above challenges in the organization helped me obtain the necessary information, and I agreed to provide them with a copy of my research upon its completion. Moving to an area with better internet speed resolved my internet connection issues and enabled me to conduct my research properly.

1.8. Structure of the thesis

There are six chapters in this study. The first Chapter introduces the background, problem description, objectives of the study, research questions, significance, scope, and limits is given in

Chapter 1, the Introduction. It provides a thorough overview of the history and importance of the research. A summary of the LST, changes in land use and cover, and the NDVI is given in Chapter 2, which is devoted to the Review of Literature. It looks at pertinent studies and the theories that are directing the current inquiry. The general research methodology, including data gathering techniques and an overview of the subject field, is covered in Chapter 3, Methodology. It describes the steps taken to collect and process the data for the study as well as the methodology. Chapter 4, Analysis and Presentation, presents the comprehensive analysis and findings from data collection and image classification. It includes land use and cover maps generated through maximum likelihood classification, as well as results from NDVI and LST analyses. This chapter also features the change analysis of LU/LC and LST, with geographical maps prepared to compare changes over time.

Chapter Five presents the discussion part and the last chapter six presents" conclusions and recommendations. In this section, key findings and critical points that need further treatment have been forwarded as recommendations.

CHAPTER TWO

LITERATURE REVIEW

2.1. Operational definition of terms

Accuracy: The degree to which a quantified value resembles the actual (true) value is known as accuracy (Walther & Moore, 2005).

Land resources: is used for describing a measurable portion of the large area of the surface. including the near-surface climate, the topography and soil types, and surface hydrology (which includes rivers, marshes, lakes, shallow, and swamps). the sedimentary strata close to the surface and the associated groundwater and hydrological reserve, the populations of plants and animals, the pattern of human settlement, and the physical remnants of both past and present human activities (roads, buildings, drainage systems, landscaping, etc.) (Briassoulis, 2009).

Land cover: The observed (bio) Land cover refers to the actual physical covering of the earth's surface. It is the ground's surface cover, including bare earth, water, plant, and urban infrastructure (Di Gregorio, 2005).

Land use: is defined by the plans, actions, and resources humans use in a particular land cover type to create, alter, or preserve it (Di Gregorio, 2005).

Temperature is an object's degree of hotness or coldness (Martin & Kline, 2004).

Urban: An urban area, built-up area, or urban agglomeration is a human settlement having a dense population and constructed environment infrastructure (McMillen & Smith, 2003).

2.2. Concept of land-use/land-cover change

The concept of LU/LC change refers to the transformation and alteration of the earth's surface as a result of human activities and natural processes over time. The term LU/LC has been used in several studies, and it refers to the ultimate resource of the biosphere land. Still, the definitions of these two phrases are distinct and they explain two different problems. Water bodies, plants, soil, and hard surfaces are all examples of the observed biophysical cover on the earth's surface which is referred to as land cover (Wulder et al., 2018). The previous few decades have seen significant human-induced changes to the earth's surface, including deforestation, agricultural practices, and urbanization. Land is the most superior resource in the biosphere, and the LU/CC concept has been combined in many studies. Land use refers to the exploitation or utilization of land by human

activities for settlements, agriculture, forestry, and grazing, affecting land surface processes such as biogeochemistry, hydrology, and biodiversity. Under this context, a change in the landscape's surface component is only deemed to have occurred if the surface appears differently upon at least two subsequent viewings (Lemlem,2007). Given this, a change in the surface component of the landscape is only regarded as having happened if the surface appears differently when viewed at least twice in succession (Smith, et.al., 2014). FAO (1999) described land use as human arrangements, actions, and inputs on a certain type of land cover with the intention of either preserving or producing change. As per (Lambin & Meyfroidt, 2010), changes in socio-economic innovations and changes that result in a significant loss of ecosystem services can have negative socio-ecological feedback, leading to a shift in LU/CC (Fasika et al., 2019). These national and international patterns highlight the intricate interactions between human activity and environmental factors that shape LU/LC dynamics. Creating sustainable land management strategies that strike a balance between economic growth, environmental preservation, and climate resilience requires an understanding of these developments.

2.3. Causes of land-use and land-cover changes

Due to human-induced factors like deforestation, agricultural practices, and urbanization, the earth's surface has undergone significant changes in recent decades (Gries et al., 2019). When land is used for habitation, farming, forestry, or pasture, it alters the biogeochemistry, hydrology, and biodiversity of the ground surface (Jansen & Di Gregorio, 2002). These alterations are influenced by people's actions, decisions, and resources utilized on specific land types to preserve or induce modifications (Sun & He, 2009). Negative socio-ecological feedback, driven by environmental changes, economic expansion, population growth, and technological advancements, significantly impacts LU/CC (Lambin & Meyfroidt, 2010). Sustainable management of these changes is essential to balance environmental preservation with human needs.

At the global level, LU/CC starts at the individual land parcel level, where land managers decide to shift to different land uses (Meyer & Turner, 1992). LU/CC involves converting one type of land cover to another and modifying conditions within a category. Population growth increases the demand for resources like food, water, energy, and living space, leading to urban sprawl, agricultural expansion, and natural resource extraction (Gashaw et al., 2014). These changes impact human populations, affecting their lifestyles, resource access, and overall well-being

(Thapa et al., 2022). Although they are influenced by local circumstances, country-specific tendencies mirror these worldwide ones. For example, Ethiopia has experienced severe LU/CC due to its rapid agricultural expansion and urbanization. The nation's expanding population is primarily responsible for the transformation of grasslands and woodlands into urban areas and agricultural land. On the other hand, policy-driven programs, like reforestation, work to improve climate change resistance and lessen environmental degradation. Developing sustainable land management strategies that strike a balance between economic development, environmental preservation, and climate resilience requires an understanding of these LU/CC dynamics at both the national and global levels (Briassoulis, 2020).

2.4. Land-use and land-cover change in Ethiopia

In Ethiopia, the availability and management of natural resources vary significantly from one place to another place. Differences in terrain, climate, and biogeography are the causes of this variability (Agarwal et al., 2002). Not only is human activity accelerating LU/LC, but it is also affecting individuals. Many biophysical resources, such as water, vegetation, soil, animal feed, and others, are altered by the dynamics of LU/CC (Ali, 2009). According to earlier research, Ethiopia has experienced significant LU/CC variations in several regions, as well as the expansion of cultivated land at the rate of forestland and undeveloped areas as an outcome of land scarcity. Agricultural methods and human habitation have a long history, particularly in Ethiopia's highlands. More recently, highland population pressure has resulted in unsustainable practices and the degradation of natural resources (Miheretu & Assefa., 2017).

2.5. Land surface temperature

Land surface temperature refers to the temperature on the surface of the earth, often described as the skin temperature of the earth's surface (Ira, 2018). The radiative skin temperature of the land surface is referred to as LST, as measured in the direction of the remote sensor (Kumar & Gonencgil, 2023). LST provides useful information about surface properties and conditions. Measuring The geographical arrangement of LST patterns is also useful for understanding various issues such as evapotranspiration, temperature change, and urban environmental conditions (Govind & Ramesh, 2019). Regarding climate change, urban heat islands, droughts, public health, and other issues, LST is a crucial environmental metric (Mo et al., 2021). Several elements

influence surface temperatures in metropolitan areas, including day length, season, winds, currents, clouds, topography, location, rural environment, land use type, building materials, and changes in urban geometry (Ibitolu et al., 2017). The replacement of vegetation and other natural surfaces by people's efforts like asphalt, concrete, and metal in urban areas leads to environmental impacts such as reduced evapotranspiration, rapid runoff, and increased surface temperature (Singh et al., 2014). Therefore, land use change and LST assessment are necessary for comfortable and sustainable cities.

2.6. Land surface temperature retrieval algorithms

Remote sensing of thermal data provides the most accurate estimates of land surface temperature (LST) over large areas, with geostationary satellites being essential for fully characterizing the LST diurnal cycle (Trigo et al., 2008). Satellite-based Thermal Infrared (TIR) data directly relate to LST through the radiative transfer equation. The quest for LST from remote sensing and TIR data has a rich history dating back to the 1970s (Li et al., 2013).

Recent advancements have seen various techniques and platforms used to retrieve LST, with a focus on examining urban LST changes over time using datasets from satellites and ground-based sources. Landsat data, particularly with its precise spatial resolution of thermal bands, has been extensively utilized for acquiring LST in urban areas and studying its spatial variations in urban landscapes (Yin et al., 2020).

LST is a critical parameter in hydrology, meteorology, and the surface energy balance obtained crucially through remote sensing at regional and global scales. The calculation of LST typically involves using Landsat 8 images, focusing on thermal bands 10 and 11, and using bands 4 and 5 for NDVI calculations. Atmospheric effects must be corrected before obtaining land surface brightness temperatures, with subsequent adjustments using spectral emissivity values to compute LST, accounting for land surface roughness, vegetation cover, soil thermal properties, and moisture content (Friedl et al., 2010).

Several algorithms have been developed to retrieve LST from satellite imagery. The single window method uses a radiative transfer equation to correct at-sensor radiance to surface radiance, followed by an emissivity model to separate surface radiance into temperature and emissivity (Schmugge et al., 1998). The split-window technique calculates surface brightness temperatures

as a linear combination of two channels, but its coefficients are only valid for the datasets used to derive them (Coll et al., 2006).

Other techniques include the single-channel algorithm, temperature/emissivity separation method, and mono-window algorithm (Ayanlade et al., 2021). The split window algorithm (SWA) is widely used to eliminate atmospheric effects by exploiting differences in atmospheric absorption between adjacent thermal infrared channels centered around 11 and 12 μm (Mirsanjari et al., 2021).

2.7. Normalized difference vegetation index

One of the first analytical products from remote sensing that was utilized to streamline the complexities of multi-spectral imagery, is now the most popular index used for vegetation assessment (Huang et al., 2021). Urban green spaces and vegetation cover play an important role in balancing human biophysical relationships and maintaining environmental quality (Roza et al., 2017). Vegetation growth conditions determine the ground temperature in a given area, as high NDVI values, indicate the low ground LST due to latent heat flow from the ground to the atmosphere via evapotranspiration. NDMI is utilized alongside NDVI to gauge surface urban heat island effects in Landsat imagery, evaluating moisture content in landscape elements via NIR and IR reflectance comparisons. It indicates higher humidity with values >0.1 (light colors) and lower humidity with values near -1 (dark colors) (Mihai, 2012). Generally, higher NDVI locations exhibit lower LSTs, as evidenced by numerous studies (Gowarda et al., 2002). Research has consistently shown that distribution patterns, vegetation type, and the percentage or density of green cover significantly reduce land surface temperature (Sruthi & Aslam, 2015; Odindi et al., 2015).

In Ethiopian contexts with low vegetation cover, land surface temperature has been observed to increase by 3–8°C from 1985 to 2015, highlighting the impact of land use changes (references needed). Furthermore, correlation analyses across Addis Ababa's sub-cities have indicated a negative relationship between land surface temperature and NDVI, underlining the cooling effect of green spaces and vegetation in urban environments (Worku et al., 2021).

2.8. Urban Heat Island

A metropolitan area is known as a UHI where temperatures are visibly higher due to human activity than in the nearby rural areas. As a result of continued urbanization, cities that habitually go

through temperatures that are higher than their surroundings are known as urban heat islands (Oke, 2017). UHI are also defined as phenomenon/events that occur when air and ST in urban areas become significantly greater than those experienced in nearby areas and land-cover change has become a central component in current strategies for managing natural resources and monitoring environmental changes (Sobrino et al., 2012). The report, that climate change has contributed to a significant increase in the global mean temperature (IPCC, 2014). There are several contributing factors, that play a major part in the creation of urban heat islands such as low albedo materials, wind-blocking, air pollutants, human gathering, distractions of trees, and increased use of air conditioners (Nuruzzaman, 2015).

2.9. GIS and RS's role in detecting the land-use/land-cover

Geographic Information System (GIS) is a comprehensive system designed to collect, store, process, analyze, organize, and display spatial or geographic data (Reddy, 2018). GIS data can be classified into two major groups: spatial data, which includes location values, and non-spatial data, which describes spatial data in tabular form (Burrough et al., 2015). According to Maguire (1991), GIS is not just a digital repository of spatial objects like areas, points, and lines, but also facilitates spatial analysis by examining the relationships between these objects based on their location and geometry.

Foresman (1998) notes that the integration of computer technology and mapping in the 1960s enabled map superimposition and overlay techniques in fields beyond cartography. This integration has exponentially increased the power of GIS by integrating climate, environmental, terrain, agronomic, economic, social, and institutional management data, providing new and powerful modeling capabilities for managers and scientists alike.

Remote Sensing (RS) is the art, science, and technology of monitoring objects, scenes, or phenomena through instrument-based techniques (Damen, 2022). Earth observation from aerial platforms has evolved significantly over the last 150 years, starting with the first balloons used for earth observation in the 1860s (Lillesand and Kiefer, 2015). RS provides data essential for analyzing temporal and spatial variations in large-scale environmental parameters, supporting applications such as crop yield estimation, environmental damage assessment, land use monitoring, urban planning, and geographic mapping for both civil and military purposes (Javed et al., 2021).

GIS and RS techniques have been widely employed globally to study historical LU/LC changes and analyze LST dynamics. RS is used for identifying vegetation cover, air pollution, LST, and other surface characteristics (Zha, 2012; Weng, 2004). Understanding the relationship between LU/LC and LST is crucial for effective land management. The availability of historical RS data, reduced data costs, and improved satellite resolution have enhanced RS's role in monitoring LU/LC changes over time. GIS and RS tools are widely applied for quantifying and estimating LST, supporting decision-making across various disciplines by providing insights into surface temperature dynamics.

2.10. Changes in land cover and use's effect on land surface temperatures

One of the primary factors contributing to the increase in LST is LU/LC change. Various researchers concur that changes in land use and the unplanned use of land resources are significant contributors to rising land surface temperatures (Oluseyi et al., 2011). Among the principal causes of this trend is LU/CC. Land use/land-cover change has a noteworthy effect on the LST, with built-up areas and fallow land experiencing the highest temperatures (Omeno et al., 2021). The conversion of LU/LC types into built-up areas has been identified as a key driver of this temperature increase.

According to research by (Oluseyi et al, 2011), there are spatial correlations with changes in the traits of different land-use classifications or categories. This study focuses on LST variations for different land uses in Anyigba Town, Kogi State, Nigeria, between 1995 and 2006. It demonstrates that the surface temperatures of the built-up area, stream, and vacant land varied and increased by 1ºC, while the vegetation and farmed land saw a rise of 0.95ºC. At different latitudes, the effects of changes in LU/LC on LST vary, For instance, in tropical and temperate regions of East and South Asia (Shukla et al., 1990). The land cover changed to grazing fields and settlement areas, as evidenced by the association between land-use changes, biodiversity, and land degradation throughout East Africa (Maitima et al., 2009).

2.11. Conceptual framework

A conceptual framework is an illustration that depicts the expected relationship between cause and effect in research. It outlines the relevant objectives of the investigation and demonstrates how they interconnect to produce logical findings. When analysis LU/LC and their correlation with

LST, a conceptual framework can be developed to understand the relationship between different variables, including LU/LC types and their impact on LST. This framework considers various landscapes such as built-up areas, dry soil, rocks, asphalt roads, concrete infrastructure, water bodies, forests, grasslands, shrublands, and cultivated land, each having distinct effects on LST. The landscape structures' coverage and state of health in different seasons are also considered in the conceptual framework. Understanding the connections between land uses, types of cover, and LST allows for the examination of how LU/LC affects LST and the identification of any relationships.

Creating a theoretical structure to evaluate LU/CC and examining how they relate to land surface temperature requires researching previous studies in the field this review helps identify relevant variables and their relationships, which can then be incorporated into the conceptual framework. The conceptual framework provides a methodical approach to understanding the complex relationship between land use, cover change, and LST. It serves as a guide for research, helping to define research questions, identify variables, and analyze the expected cause-and-effect relationships.

CHAPTER THREE

MATERIALS AND METHODS

3.1 Description of the study area

3.1.1.Location

Asella and its surrounding areas are located in the Arsi Zone, of the Oromia region in Ethiopia. It is 168.5km away to the southeast of Ethiopia's capital city, Addis Ababa. The research region, which covers a total area of 961.01$Km^2$is located between latitude and longitudes of 7° 54' 0"-8° 15' 0" N and 38° 15' 0"-39° 14' 0" E, (Fig.3.1). It is located in the Ethiopian highlands found in the southeast of the country's center. The altitude of the area ranges from 1620 m to 3868 m above sea level and it is located. Asella town serves as the seat of the Arsi Zone administration. It was previously the capital city of the Arsi Province until it was demoted to the zone of Oromia following the adoption of the 1995 FDRE constitution.

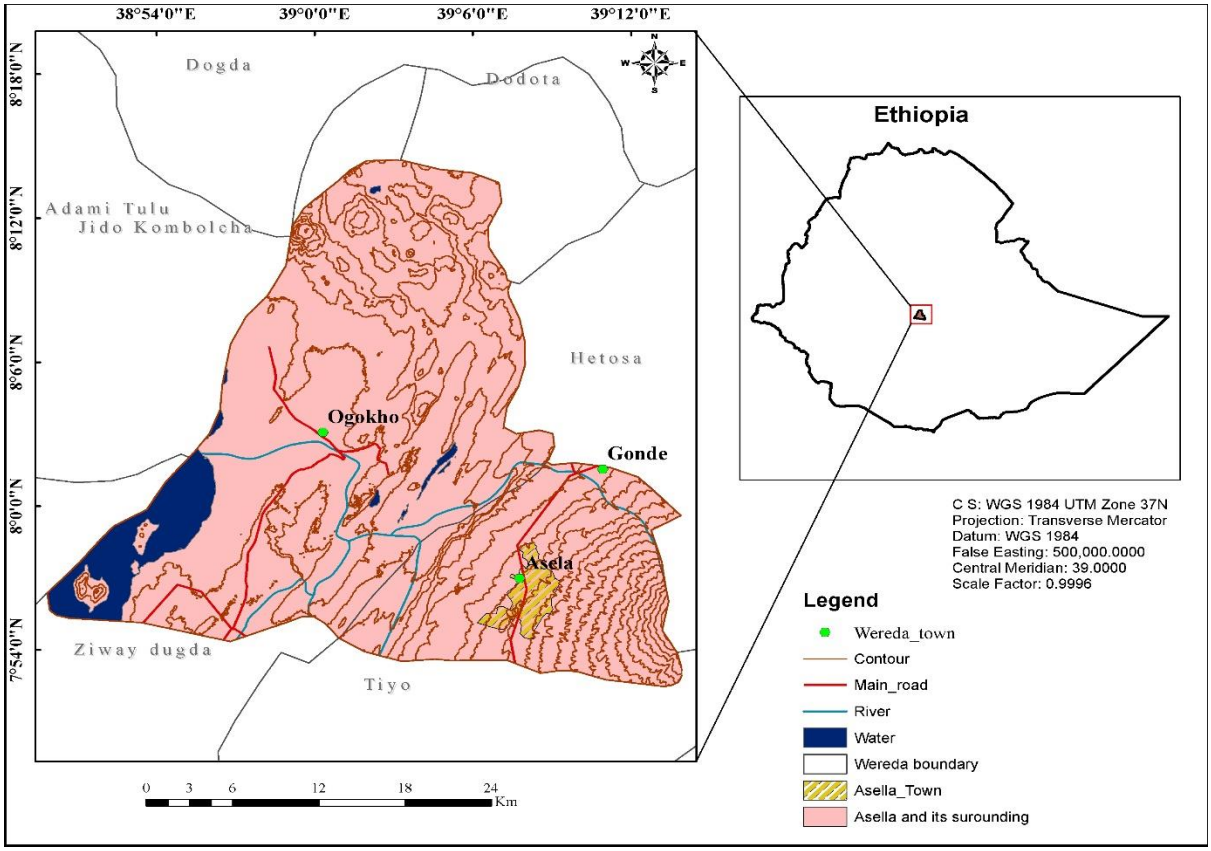

Figure 3. 1: Location map of the study area.

3.1.2. Topography

Topography is the study of the earth's surface features, focusing on the shape, characteristics, and related phenomena of the land. It encompasses landforms, elevation, latitude, longitude, and the creation of topographic maps. Topographic mapping utilizes latitude and longitude coordinates to accurately pinpoint structures on the earth's surface. These maps offer detailed terrain representations, highlighting features such as hills, valleys, and other relevant information. Understanding topography is crucial for comprehending landscapes' physical characteristics and spatial distribution, with applications in geography, geology, environmental science, and engineering.

The study area features slopes ranging from 0º to 75.7º, with the western region characterized by dark green areas, and the eastern and northwest ridge sections also displaying varied slopes. The southeast part reaches the highest elevation at 3868m, while the lowest point is 1620m. These geographic variations result in significant altitude differences, particularly noticeable in the southeast. Figures 3.2a and 3.2b visually represent the slope and elevation distribution across the area.

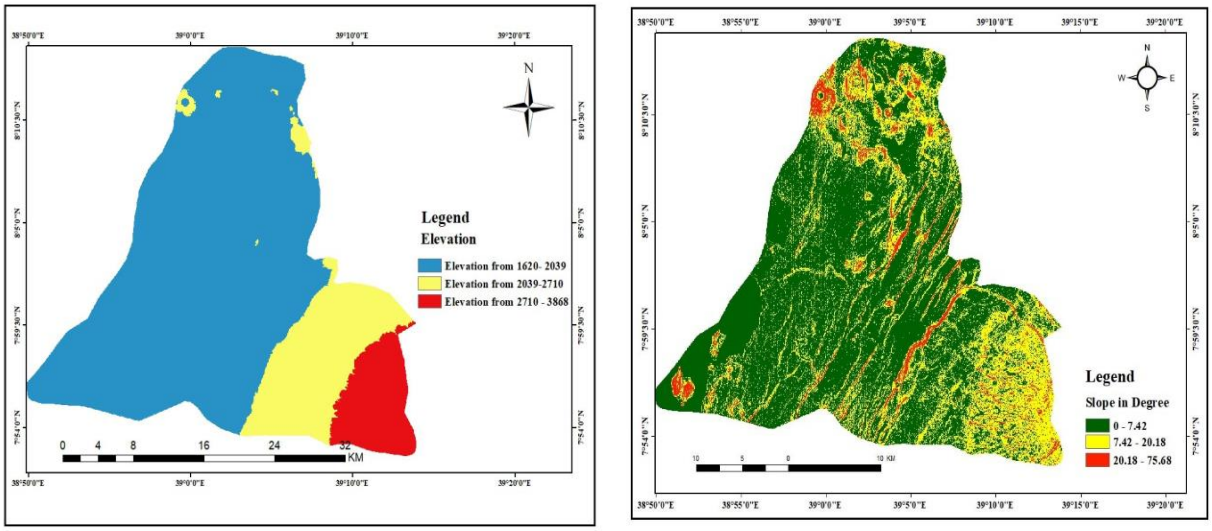

Figure 3. 2: (a) Elevation map and (b) Map of the Study Area's slopes

3.1.3.Climate

In terms of climate classification, Asella and its surroundings fall into the Köppen-Geiger category of subtropical highland climates (CBW) Climate-Data.org. at a height of 2356.7 m above sea level, The climate of Asella and its surrounding area is classified as tropical wet and dry, or savanna (Aw). The district experiences 15.47ºC (59.85ºF) annually. Its elevation and proximity to the equator are the reasons for this classification. Consequently, there is little monthly temperature variance in the town.

The main factor separating the seasons in the study area is the amount of rainfall, which is highest in August and lowest in December. The impact of height and minimal temperature fluctuation provides for a rather steady climate throughout the year.

A. Rainfall

A long-term rainfall record from 1993 to 2022 at the meteorological station shows an average annual rainfall in the research area's maximum dispersion from 1993 to 2022 was 1434.4 mm whereas the minimum is 922.2 mm with the maximum and minimum of the monthly average rainfall of 222 mm in July and 22.7 mm in December, respectively (Fig.3.4).

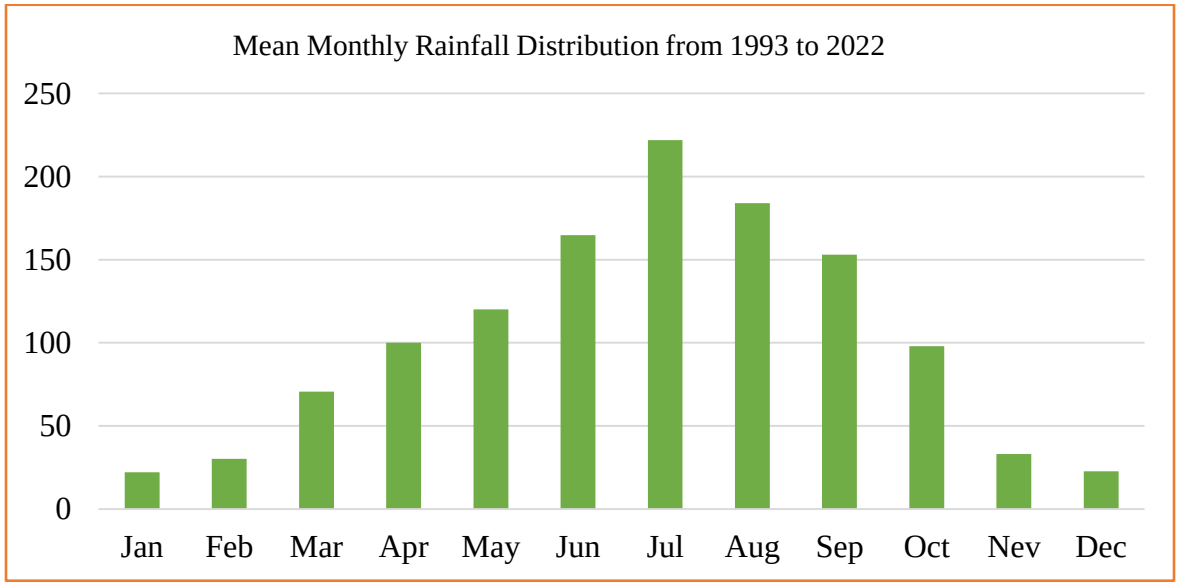

Figure 3. 3: Distribution of the Study Area's monthly mean precipitation.

The average rainfall recorded in 1993 was 10568 mm and in 2003 was 1438.8 mm, while in 2005 and 2020 it was 1075.6 mm and 323.1mm in 2022 detain information in (fig. 3.5).

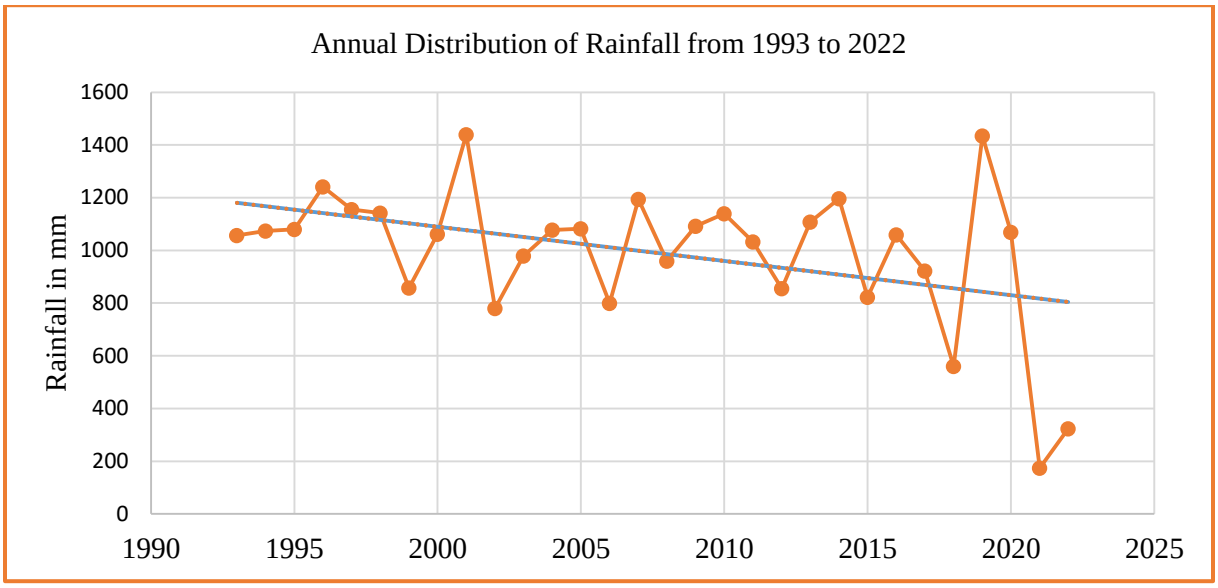

Figure 3. 4: Annual distribution of rainfall from 1993 to 2022.

B. Temperature

The monthly mean maximum and minimum temperatures of the Asella town and it is surrounding are 28.9 °C in February and 10.9 °C in November.

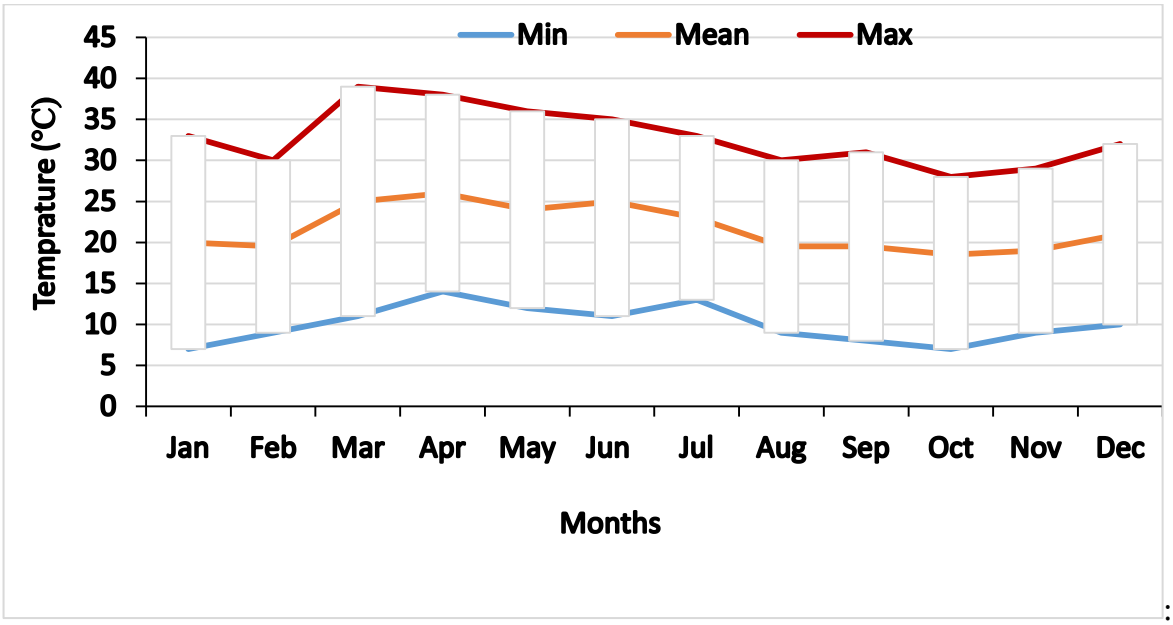

:

Figure 3. 5 Maximum, minimum and mean monthly Temperature during 1993–2022.

C.Vegetation

The distribution of vegetation in the area is mostly influenced by the local climate. The research region has a weyina dega and dega climate. In these weather conditions, vegetation is scarce, and typical examples found in the area are shrubs and scattered trees of eucalyptus. Eucalyptus trees are grown by local communities that have soil conservation programs applied in the main part of the study areas. The local people cultivate some types (of crops) in the region, like as teff, wheat, barley, and maize. The harvest season is in October and December when the rain is deficient.

3.1.4. Population

Ethiopia conducted its third national census of population and housing in 2007. As per CSA 2007, the combined population of Asella and its environs was 263,861 in 2007. In this group, there were 131,596 (49.87%) women and 132,265 (50.13) males.

According to the official estimate from the Ethiopian Statistics Service, the projected population of Asella and the environs in 2017 is 337,277 people. Out of this, 168,104 were male and 169,173 were female This projection is based on various variables and assumptions of the population density. The detailed information is presented in (Fig.3.7.)

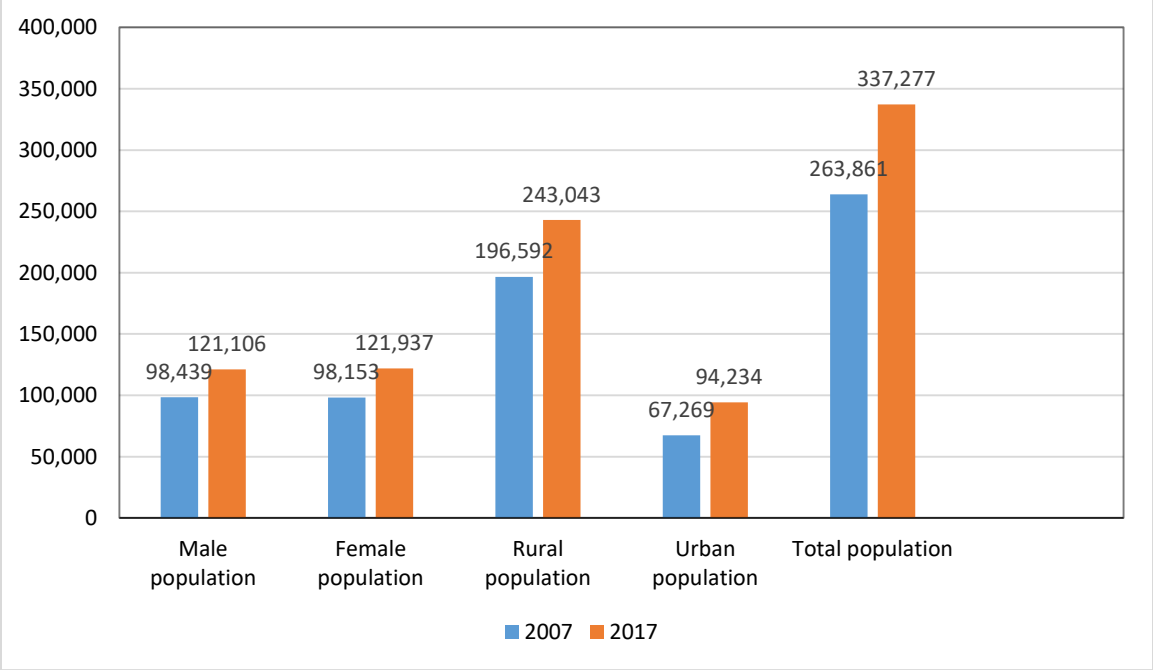

Figure 3. 6: Population of Asella and its surrounding areas.

3.2. Data and software

The research methodology used a dual approach to ensure thorough evaluation using both sources of primary and secondary data. The primary data, which came primarily from satellite imagery, served as the investigation's mainstay and provided direct, first-hand information that was essential to the study objectives. Using data from satellites allowed for the thorough study and observation of relevant factors, providing insights into dynamic spatial or environmental phenomena. Secondary sources of information from governmental and non-governmental organizations and publicly available data complemented the primary data. These secondary data streams enhance the evaluation by providing background information, datasets for comparison, or supporting evidence for the conclusions drawn from the primary data.

By combining primary as well as secondary data sources, a thorough grasp of the issue was obtained, which increased the validity and depth of the study's conclusions. Ancillary data from various sources was used to add layers of data to the core dataset that were required for a comprehensive evaluation. Ancillary data in the research domain provide a range of viewpoints and additional insights.

3.2.1. Primary data

Satellite images from the well-known Landsat program serve as the main dataset for this research and provide an important insight into how the earth's surface changes over time. Three different Landsat sensors were used in the research: the Thematic Mapper TM in 1987, the Operational Land Imager/Thermal Infrared (OLI/TIRS) in 2023, and the ETM+ in 2005, which made it easier to gather multispectral data over a wide variety of spectral bands. This made it easier to conduct a more thorough analysis of many aspects of the land cover, such as the pattern of urban growth, the division of land cover, and The geographical arrangement of vegetation. Later, the 2005-introduced ETM+ sensor outperformed its predecessor by providing increased spatial resolution and spectral bands, allowing for a more detailed assessment of change detection and land classification.

The combination of OLI and TIRS sensors yielded a comprehensive comprehension of the earth's surface, as OLI collected optical and near-infrared wavelengths while TIRS concentrated on thermal infrared radiation. Due to this dual capability, the study was able to investigate a variety of topics, including changes in LST, the health of vegetation, and the identification of land cover

features. The study used DEM data in their investigation in addition to the satellite images. With its 12.5m x12.5m spatial resolution, the DEM dataset offered vital details on the research of the slope and elevation of the area. Using elevation values to represent the terrain, we were able to create topographic maps that revealed the subtleties of the highs and lows in the environment. These topographic insights improved our understanding of landscape dynamics by helping landform analysis, hydrological modeling, and slope evaluation. Additionally, field data-gathering activities were crucial in completing the remote sensing datasets. Validate and improve the data derived from satellites, this required the painstaking recording of exact GPS coordinates at predetermined sites inside the study region. Furthermore, the researchers took on-location photos that documented several LU/LC categories, such as agricultural areas and dense woods, as well as urban infrastructure and water bodies. The study's results were more accurate and thorough since these photos provided useful visual assistance for recognizing and categorizing various landscape elements. Essentially, the combination of observations in the field, DEM data, and Landsat satellite imagery created a strong framework for assessing land cover dynamics, enabling researchers to fully understand temporal trends and spatial patterns inside the study area.

3.2.2. Remote sensing data acquisition

As shown in Table 3.1, LST, NDVI, and LU/CC were calculated using remote sensing imagery in Asella and its surrounding areas. Thermal infrared sensors, which gather radiation released by the earth's surface and translate it into temperature data, are the source of LST values. To assess the quality and quantity of vegetation, multispectral data—especially red and near-infrared bands—is used to construct the NDVI, or vegetation index. In addition, LU/CC classification was carried out using GIS methodologies and classification algorithms to quantify the extent of each land cover class within the study area. This included classifying land cover categories such as agricultural land, urban areas, forests, and water bodies.

Table 3.1 Sources-related remote sensing data.

Date of Acquisition	Data sets and sensor	Path	Row	Multispectral Band	Thermal Band	Source	Spatial Resolution (Termal bads)	Spectral Range (micrometers)
1987-02-09	Landsat 5TM	168	054	1 to5 and7	6	USGS	120m	10.45-12.45
2023-02-18	Landsat 7ETM+	168	054	1 to5 and7	6	USGS	60m	10.45-12.51
2023-02-12	Landsat 8OLI/TIRS	168	054	1 to7	10 and 11	USGS	100m	10.60-12.51

To compute LST, NDVI, and LU/CC in Asella and its surroundings, as shown in Table 3.1, remote sensing imagery including data from the multispectral band, as shown in /Fig 3.8/, was utilized. LST values are temperature readings obtained from thermal infrared sensors that detect radiation emitted from the earth's surface. The state of health and density of the vegetation was evaluated by computing the NDVI using multispectral data, especially the red and near-infrared bands. Furthermore, the study region underwent LU/CC classification to classify various land cover types, including agricultural land, urban areas, woods, and water bodies. This was achieved by employing GIS techniques and classification algorithms to measure the amount of each land cover class.

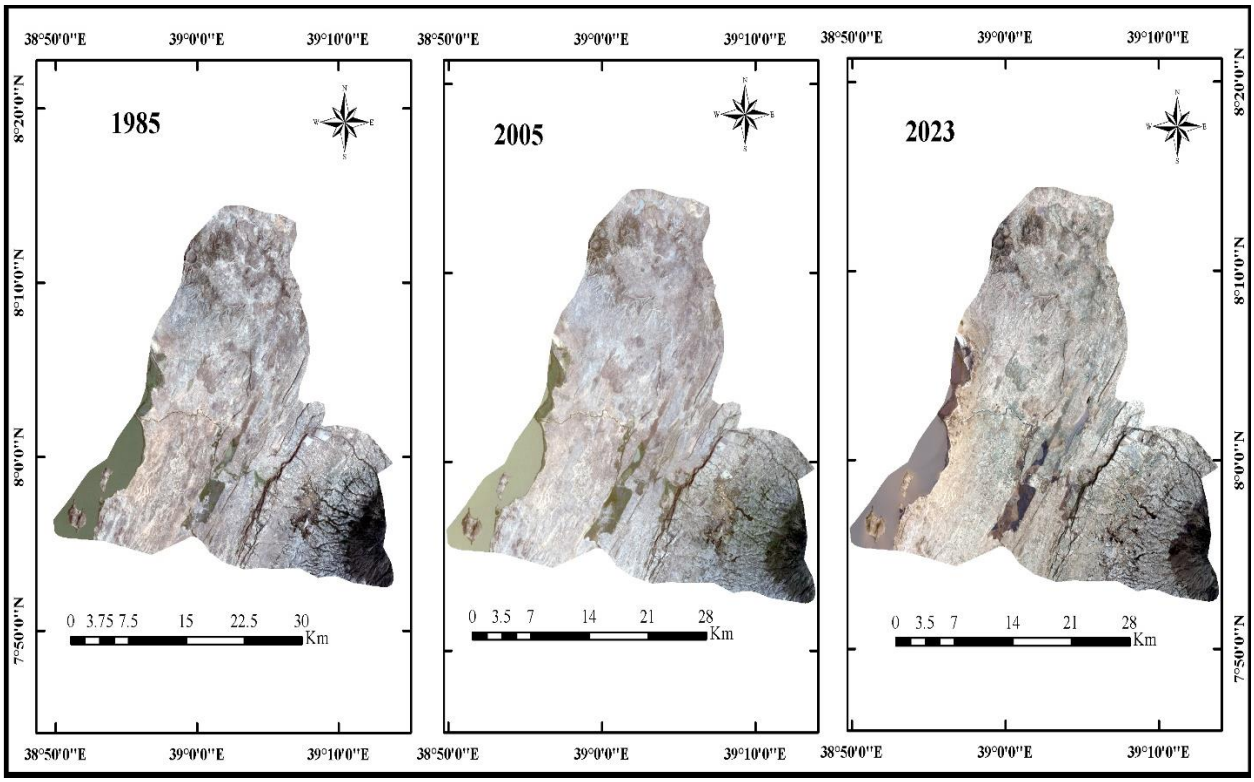

Figure 3. 7: Landsat Images of 2023 OLI and This technique, 2005 ETM+, and 1987 TM.

A. Landsat thematic mapper (TM)

The TM sensor, a crucial component of the Landsat program, was fitted aboard the Landsat four and five satellites. It was eventually retired in May 2012, having served an amazing 30-year existence from July 1982 to that date. Over a three-decade period, systematic and comprehensive earth observations were made possible by the 16-day repeat cycle of the TM sensor, which yielded invaluable insights into the dynamics of the planet's environment.

Sophisticated features characterize the TM sensor. It has seven spectral bands, three of which are visible and four of which are infrared. Nuanced observations on the earth's surface features, vegetation health, changes in land cover, and other factors were made possible by this configuration's many facets. Because of its precise tuning to thermal infrared radiation, Band six of the TM sensor was particularly noteworthy. This spectral band plays a key role in measuring variations in surface temperature across different landscapes. Surface temperature is a crucial factor for understanding climate patterns, the effects of urban heat islands, and the dynamics of ecosystems.

The Landsat TM sensor has been instrumental in furthering scientific understanding and environmental monitoring during its operational lifetime. With a wealth of data essential for global policy formation, resource management, and scientific research, its legacy as a cornerstone of remote sensing technology continues to this day. Full details are displayed in Table 3.2.

Table 3.2 lists sensor bands and descriptions of Landsat 5 Thematic Mapper.

Landsat5 Thematic Mapper (TM)	Bands	Description	Wavelength Range (µm)	Spatial resolution(m)	Repeating time	Source
	Band 1	Blue	0.45 - 0.52	30	16 days	USGS
	Band 2	Green	0.52 - 0.60	30		
	Band 3	Red	0.63 - 0.69	30		
	Band 4	Near Infrared	0.76 - 0.90	30		
	Band 5	Shortwave Infrared 1 (SWIR-1)	1.55 - 1.75	30		
	Band 6	Thermal Infrared	10.40 - 12.50	120		
	Band 7	Shortwave Infrared 2 (SWIR-2)	2.08 - 2.35	30		

B. Landsat 7 enhanced thematic mapper plus (ETM+)

Since July 1999, the Landsat ETM+ sensor, which is part of the Landsat 7 satellite, has taken images of the planet almost constantly, repeating every 16 days. Taking regular, very detailed, high-quality images of the surface of the earth is its goal. After operating practically continuously for 20 years, Landsat 7ETM+ has shown to be an important source of knowledge for a variety of uses, such as urban planning and environmental monitoring.

Among its distinctive features is the 16-day repetition cycle of the Landsat 7ETM+ sensor, which allows it to systematically and regularly return to the same areas of interest. This periodicity makes

it possible for researchers and decision-makers to precisely track changes over time in the environment, land use, and cover. The imagery obtained by the Landsat 7ETM+ sensor comprises eight spectral bands, each offering a unique viewpoint on a different region on the earth's surface. Data with a 30m spatial resolution are available for bands 1 through 5 and 7, which provide comprehensive details about the health of vegetation, geological features, and other characteristics of the land cover. Monitoring changes in vegetation dynamics and classifying land cover are two applications that benefit greatly from this resolution.

The Landsat 7ETM+ sensor has additional bands in addition to these regular bands: band 6 for thermal imaging and band 8 for panchromatic imaging, each with unique features. Band 6 of the TM sensor absorbs thermal infrared radiation from the earth's surface, enabling the identification of thermal anomalies such as volcanic eruptions and urban heat islands through temperature fluctuations and activity. Band 6 offers important insights into surface temperature trends and energy fluxes with a 60m spatial resolution. With a remarkable resolution of 15 meters, band 8 provides the highest spatial resolution of all the Landsat 7ETM+ bands. Applications requiring in-depth visual interpretation, such as infrastructure building, disaster response, and urban planning, are especially well-suited for this panchromatic spectrum. Its exceptional resolution makes it possible to distinguish fine-scale details and accurately draw boundaries, which makes it a vital tool for mapping and analysis. Full details are displayed in Table 3.3.

Table 3. 3: Bands and Description for Landsat 7ETM+.

Satellite /sensor	Bands	Description	Wavelength Range (µm)	Spatial resolution (m)	Repeating time	Source
Landsat 7 Enhanced Thematic Mapper Plus (ETM+)	Band 1	Blue	0.45 - 0.52	30	16 days	USGS
	Band 2	Green	0.52 - 0.60	30		
	Band 3	Red	0.63 - 0.69	30		
	Band 4	Near Infrared - NIR	0.77 - 0.90	30		
	Band 5	Mid-Infrared - MIR)	1.55 - 1.75	30		

	Band 6	Thermal Infrared - TIR)	10.4 - 12.5	60		
	Band 7	Mid-Infrared - MIR	2.08 - 2.35	30		
	Band 8	Panchromatic	0.52 - 0.90	15		

C. Thermal infrared sensor and operational land imager of Landsat 8

Launched on February 11, 2013, Landsat 8 is a sophisticated imaging system with nine spectral bands, each of which provides valuable knowledge about the surface of the earth. With a 30 m spatial resolution for bands 1-6, 9, and TIRS, precise observations of terrain features are guaranteed. Two new bands—10 and 11—among the improvements provide greater thermal imaging capabilities, supporting surface temperature variations and environmental change research. Furthermore, the advent of band 1, often known as ultra-blue, is beneficial for aerosol and coastal studies, allowing for more accurate observation of atmospheric conditions and coastal dynamics.

In addition, Landsat 8 adds band 9, which is dedicated to cirrus cloud detection, improving the satellite's capacity to recognize and assess clouds at high altitudes. Increasing our understanding of cloud dynamics and how they impact the earth's climate system requires this development., as well as raising the accuracy of weather forecasting models. With these enhancements, Landsat 8 continues to be an essential tool for academics, researchers, and policymakers, allowing unprecedented levels of precision and detail in in-depth analyses of the earth's surface and dynamic processes. Full details are displayed in Table 3.4.

Table 3. 4: Lists the bands and descriptions for the Landsat 8 OLI/TIRS.

Satellite /sensor	Bands	Description	Wavelength Range (µm)	Spatial resolution (m)	Repeating time	Source
Landsat 8 OLI/TIR	Band 1	Coastal/Aerosol (ultra-blue)	0.433 - 0.453	30	16 days	USGS

S	Band 2	Blue	0.450 - 0.515	30		
	Band 3	Green	0.525 - 0.600	30		
	Band 4	Red	0.630 - 0.680	30		
	Band 5	Near Infrared (NIR)	0.845 - 0.885	30		
	Band 6	Shortwave Infrared 1 (SWIR1)	1.560 - 1.660	60		
	Band 7	Shortwave Infrared 2 (SWIR2)	2.100 - 2.300	30		
	Band 8	Panchromatic	0.500 - 0.680	15		
	Band 9	Cirrus	1.360 - 1.390			
	Band 10	Thermal Infrared 1 (TIRS)	10.60 - 11.19	100		
	Band 11	Thermal Infrared 2 (TIRS)	11.50 - 12.51	100		

3.2.3. Field data

This work utilized GPS data as field data to verify and evaluate the accuracy of LU/CC-categorized images in different classes. After generating random points using a systematic method, field GPS point collection and picture documentation showcasing various LU/CC classes were conducted. These field observations ensured the quality and reliability of the categorized images by serving as ground truth for validation and accuracy assessments. The random points were generated to provide an unbiased and representative sample of the study area, covering diverse land use and land cover categories. This approach helps in accurately assessing the classification performance by comparing the classified data with the actual conditions observed on the ground.

3.2.4.Secondary data

The average monthly temperature and average monthly rainfall from 1993 to 2022 respectively, are two examples of secondary data that were extensively employed in the study. These datasets were essential for assessing and confirming the results. Additionally, the Ethiopian Geological Survey provided a geological map that provided important context for understanding the research area's geology. Furthermore, the CSA population data added vital demographic details that enhanced our comprehension of population dynamics within the purview of the study. The study was able to thoroughly examine the environmental, geological, and demographic elements influencing the study area by combining this disparate information, which allowed for reliable results and well-informed decision-making processes.

3.2.5.Data description and source

Data description involves summarizing and presenting key characteristics of a dataset to facilitate understanding and analysis. At the same time, source refers to the origin or the place from which the data was obtained, providing important context for its interpretation and use. Table 3.5 indicates where this investigation's primary and auxiliary data were gathered.

Table 3. 5: Data description and source used in this study.

GIS Data layer	Data Description	Data source
Vector (polygon)	Woreda Boundary	Ethio-GIS
Vector (line)	River,Contour and Roads	CSA,2008
Vector (point)	Major Town	Ethio-GIS
Raster	Elevation and Slope	DEM 12.5m from SSGI
Attribute table	Rainfall and Temperature	National Metrological Agency
Attribute table	Population	CSA,2007
Raster	Satellite Image 1987 Landsat4 TM 2005 Landsat7ETM+ 2023 Landsat 8 OLI & TIRs	USGS 1987,2005 and 2023 (Image courtesy of the U.S. Geological Survey)
Ground truth	Google Earth pro	Google Earth pro

3.2.6. Software packages used

ArcGIS 10.8 was utilized for image analysis, LST, NDVI, and map preparation in this work. ERDAS Imagine 2015 and ArcGIS 10.8 were employed for remote sensing applications, such as image enhancement, preprocessing, and LU/CC classification. Top-of-atmosphere correction, change detection, and export to Google Earth Pro.

Additionally, results can be verified and compared with ground truth using Google Earth Pro, particularly for the LU/CC verification for 1987, 2005, and 2023. Quantum GIS (QGIS): Neighborhood analysis and map algebra are two open-source programs that were utilized for raster editing. ENVI software is also utilized for categorization to compare and contrast the outcomes, in addition to ERDAS Imagine software.

Microsoft Word, Excel, and PowerPoint were used for creating Word documents, managing databases, creating graphs, and doing spreadsheet analyses.

3.3. Methods

The Earth Explorer website (USGS) provided Landsat images for 1987, 2005, and 2023, while https://libra.developmentseed.org provided Landsat 8 imagery. These sources served as the first step in the study technique. The availability of data played a role in the selection of these particular years. The images that were obtained or downloaded were deliberately selected to avoid excessive cloud cover and to align with the dry season. This method made sure that the analysis procedure was reliable and consistent. The study's overall methodological flow is depicted in Figure 3.9.

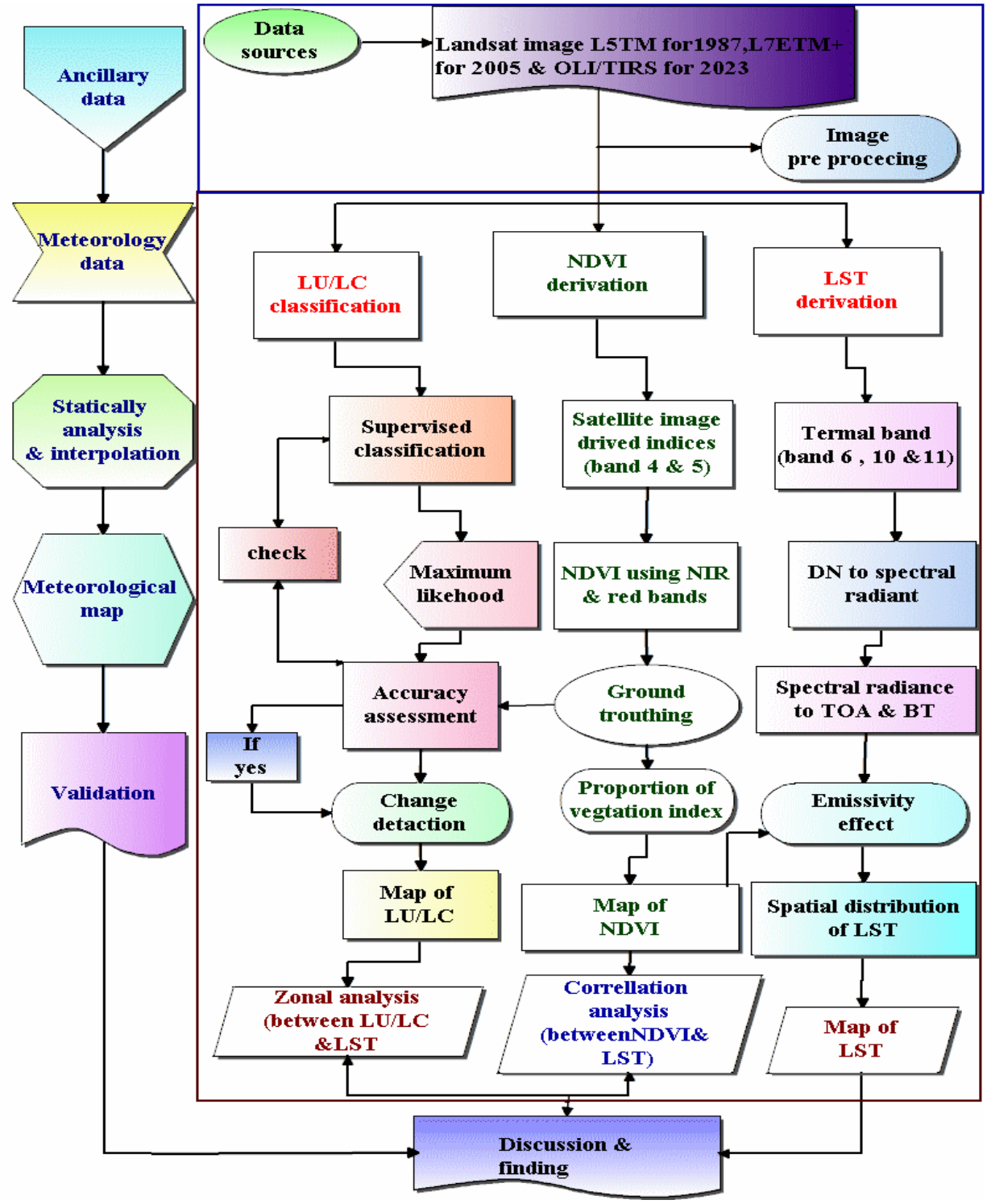

Figure 3. 8: also offers a visual depiction of the processes that were sequentially completed to meet the research objectives.

3.3.1.Data preparation and analysis

There is always distortion, noise, haze, and stripes in satellite images. Therefore, pre-processing actions were carried out before data processing. These included the following: importing, stacking layers, lowering the image to fit within the bounds of Asella and its surrounding areas, geometric correction, radiometric correction, removal of stripes, pan sharpening, and a host of other image optimization methods. In radiometric correction, air noise is removed to improve the representation of ground truth conditions from sensor data. All of the above-listed actions were done to improve the apparent contrast between scene elements, which in turn improved the image's visual interpretability.

Moreover, the study boundary was used to georeference the image. Consistency was maintained by using the Adindan coordinate system, Zone 37N for both vector and raster data in the research area over the georeferencing and reprojection processes. Ethiopia uses Zone 37N of Adindan UTM as its local datum, which guarantees consistency in spatial referencing.

3.3.2.Digital Image Processing

By correcting distorted or inferior image data, these processes seek to improve the image's usability for further alteration and produce a more accurate portrayal of the original scene. To do this, raw image data must first be processed to eliminate noise, calibrate radiometric data, fix geometric deformities, and modify the image extent via sub-setting or mosaicking. Computers are used to modify and interpret digital images, which are numerical representations of two-dimensional scenes made up of pixels. Digital image processing has traditionally been used in remote sensing for two main purposes: processing picture data for computer-assisted interpretation and improving information for human interpretation. Increasing an object's spectral separability within an image is the main objective of digital image processing operations.

3.3.3. The Landsat 7ETM+ scan-line corrector error

Data classified as SLC-off are images from Landsat 7 ETM+ acquired after May 31, 2003, the day of the Failure of the Scan Line Corrector (SLC) are known as SLC-off data. The imaging had gaps in the scan lines due to the SLC failure, which made it less suitable for some applications, especially ones that needed continuous data coverage. When the proper geometric and radiometric corrections are applied, these SLC-off data can still be beneficial for various applications.

To maintain uniformity and accuracy in reflecting the true reflectance or radiance of the earth's surface, radiometric correction entails modifying the pixel values. To provide accurate spatial representation, geometric correction entails correcting the image to remove distortions brought on by sensor and platform features.

Despite the SLC failure-related data gaps, Landsat 7 SLC-off data can still provide valuable information for various applications, such as change detection, environmental monitoring, land cover classification, and land use analysis. Users need to implement the necessary safety precautions and be aware of the limitations posed by the gaps in the data while evaluating and interpreting it.

3.3.4. Image enhancement

The method by which a technique to image data to improve its display or recording for later visual interpretation is known as image enhancement. Image enhancement often entails methods for improving the scene's visual feature differentiation (Billah and Rahman, 2004). Making images easier for people to understand or to utilize as input for automated image processing techniques is the primary objective of image enhancement, which is a crucial step in the digital image processing pipeline. A picture's visual quality can be improved by using several enhancement techniques, like contrast stretching, histogram equalization, and spatial filtering, which make it easier for human observers to perceive and understand important details.

Improved photos can also give more reliable input for later automated analysis, making it easier for algorithms to find and extract important information. Subtle details can be brought to light, noise can be minimized, and overall image quality can be improved by image enhancement, which will ultimately produce more accurate and trustworthy results from image interpretation and analysis.

3.3.5. Image classification

Sorting each pixel in a digital image into a different land cover class, or theme, is the classification process. Then, using these classified data, one may create summary statistics of the areas covered by each category of land cover or create themed maps of the land cover shown in a picture to ascertain the research area's LU/CC, GIS, and ERDAS imagine supervised The classification technique employed was the maximum likelihood approach. The supervised classification method

with a maximum likelihood (MLC) algorithm, is the most accepted classification method used in RS data (Kamusoko, 2022) The reflectance statistics for individual pixels are used in image classification. Pixels were arranged into clusters, which are groups according to their reflectance characteristics. The users decide which bands to use and how many clusters to create. The picture categorization software creates clusters based on this data. Supervised classification techniques are employed in this study.

A). Supervised classification

In the field of remote sensing, supervised classification is a reliable and popular method in light of the quantitative analysis of picture data. It is predicated on the idea that because of differences in their reflectance characteristics, various earth surface features show distinct spectral signatures in remotely sensed pictures. These spectral characteristics act as fingerprints, allowing different features to be identified from one another. Each year's supervised classification involved categorizing pixels into LU/LC classes using 40 training sites for bare land, farmland, shrubland, and settlement, and 25 sites for plantation and water body types. Verification through field assessments ensured the accuracy of LU/LC classifications based on distinctive signatures in digital images, following (Coppin and Bauer 1996).

The initial action in the procedure is gathering training samples, which are ground-level representations of each class or interest category (such as different forms of land cover). The spectral variability within every class ought to be captured by these training samples. Many remote sensing software packages have an image classification toolbar that makes it easier to create and choose training examples by letting users interactively specify areas that match several classes straight on the picture. The next stage is to use the training samples to train a classification algorithm after they have been gathered. Neural networks, Random Forests, Support Vector Machines, and Maximum Likelihood are examples of common algorithms. While training, the algorithm constructs a classification model by acquiring knowledge of the spectral signatures linked to every class. Following training, the classifier is applied to the full image, classifying each pixel according to its spectral similarity to the training samples, therefore placing it in one of the predetermined classes. Pixel-based classification is the term used for this procedure. As a result, an image is classed, with labels identifying each pixel's class. It is possible to extract useful information from remotely sensed pictures through supervised categorization. It is compatible with

numerous applications, including land-use planning, agriculture, forestry, urban development, and environmental monitoring, by recognizing and mapping diverse land-cover types or other properties of relevance. However, the standard and applicability of training data, the algorithm used for the classification, and the preprocessing techniques used on the imagery (such as atmospheric correction and radiometric calibration) all affect how well-supervised classification works. Additionally, by contrasting the categorized outcomes containing foundation truth data or higher-resolution images, validation techniques are frequently utilized to assess the correctness of the results.

Bands 1 through 7 of the preprocessed pictures were used to map the land-use/land-cover pattern using multispectral bands from bands 1 to 5 and 7 for TM 1987 ETM+ 2005 and OLI 2023. This was done by supervised classification using the likelihood classification algorithm of the ERDAS Imagine 2015 program and accuracy assessment in ArcGIS software. When it comes to supervised classification, the user-specified kinds of LU/LC classes are classified with the aid of image processing techniques. farmland, bare land, settlement, shrubland, forests, as well as water bodies were the six main classes studied in Asella and its surrounding areas. The creation of information classes and self-assessment through training sites were benefits of the supervised classification. Conversely, though, information classes might not coincide with spectral classes, and information class signature homogeneity and uniformity might differ**.** when correct to preprocess data, apply spectral enhancement techniques like principal component analysis (PCA) or spectral unmixing to improve the spectral differences between classes, thereby enhancing the distinction between information and spectral classes. Additionally, reduce noise in the spectral data using filters or algorithms to make the classes more distinguishable.

B). Maximum Likelihood Classification

In remote sensing, MLC is a popular technique for classifying pixels. MLC helps classify overlapping signatures by assigning a pixel to the most fitting class or group based on statistical decision metrics. This approach, which places pixels in the class with the highest probability, outperforms parallelepiped categorization in terms of accuracy. The disadvantage of it is that computational extraction is slower. When allocating cells to one of the classes listed in the signature file, the MLC classification tool considers the variations in class signatures.

C). Ground truthing

In the study area, a ground-truthing activity was conducted to validate various LU/LC classes. This involved verifying different types of terrain, such as farmland, scrubland, water bodies, bare land, and settlements, both urban and rural. These observed LU/LC classes were crucial in developing accurate map legends. Additionally, with the aid of GPS technology, data for the training set used in image classification was collected.

During the ground-truthing process, photographs of significant scenes and coordinates representing sampled LU/LC classes were meticulously captured. This meticulous approach ensured that the data collected was reliable and representative of the diverse landscapes within the study area. Through this comprehensive validation process, the study could effectively establish the groundwork for accurate mapping and classification of the region's LU/LC.

3.3.6.Classification Accuracy Assessment

Documenting the categorical precision of the classification outcomes is crucial after the land cover categorization process. Until the correctness of a classification is evaluated, it remains incomplete. Making a classification error matrix, additionally referred to as a confusion matrix or a contingency table, is among the most popular ways to describe classification accuracy. Error matrices compare the outcomes of an automated classification process with known reference data, or ground truth, on a category-by-category basis. To evaluate how accurate the findings of the classification are, representative points from each category of land cover will be included in a confusion matrix.

The LU/LC classification accuracy was assessed using Google Earth and the field survey. For the years 1987, 2005, and 2023, the classification accuracy's ultimate output was determined by a map of land cover and use.

A comprehensive comprehension of the research area's biological and geographical context is necessary to identify and categorize the LU/LC. A comprehensive comprehension of the region is necessary to interpret the features that are seen using Google Earth Pro and field observations. Once the Google Earth Pro version of 7.3.3.7786 was verified, six prominent LU/LC classes were identified, each of which embodied unique aspects of the topography's composition and use patterns. The foundation for later analysis and categorization projects is laid by these classes.

Table 3. 6: Lists the kinds of LU/LC along with a description of each

LU/LC classes	Description
Shrubs land	Scrubland: Less thick than forests, these regions are defined by shrubs, bushes, and small trees scattered with patches of crabgrass. The trees usually produce little useful wood.
Farmland	This term refers to spaces where annual and perennial crops are grown as their primary usage. A combination of small rural farms and expansive agricultural fields may be seen in the landscape.
Settlement	These sites include residences, workplaces, and including buildings used for business, residential, and industrial purposes. It includes a system of highways, urban facilities, and transportation infrastructure.
Waterbody	Ponds, lakes, rivers, and other man-made and natural water bodies, envelop these regions. They are essential to maintaining aquatic habitats and supplying water for many human uses.
Bare land	Beaches, dunes, exposed rocks, and salt flats are examples of non-vegetated landscapes that fall under barren land. It also includes degraded areas with rocky outcrops and eroded soil and sites and quarries.
Forest	Trees of various densities and species predominate in these areas. Timber resources, biodiversity preservation, and carbon sequestration are just a few vital ecological services that forests offer.

The steps or processes that were followed to classify land use/land cover from a Landsat image are presented in Fig 3.10.

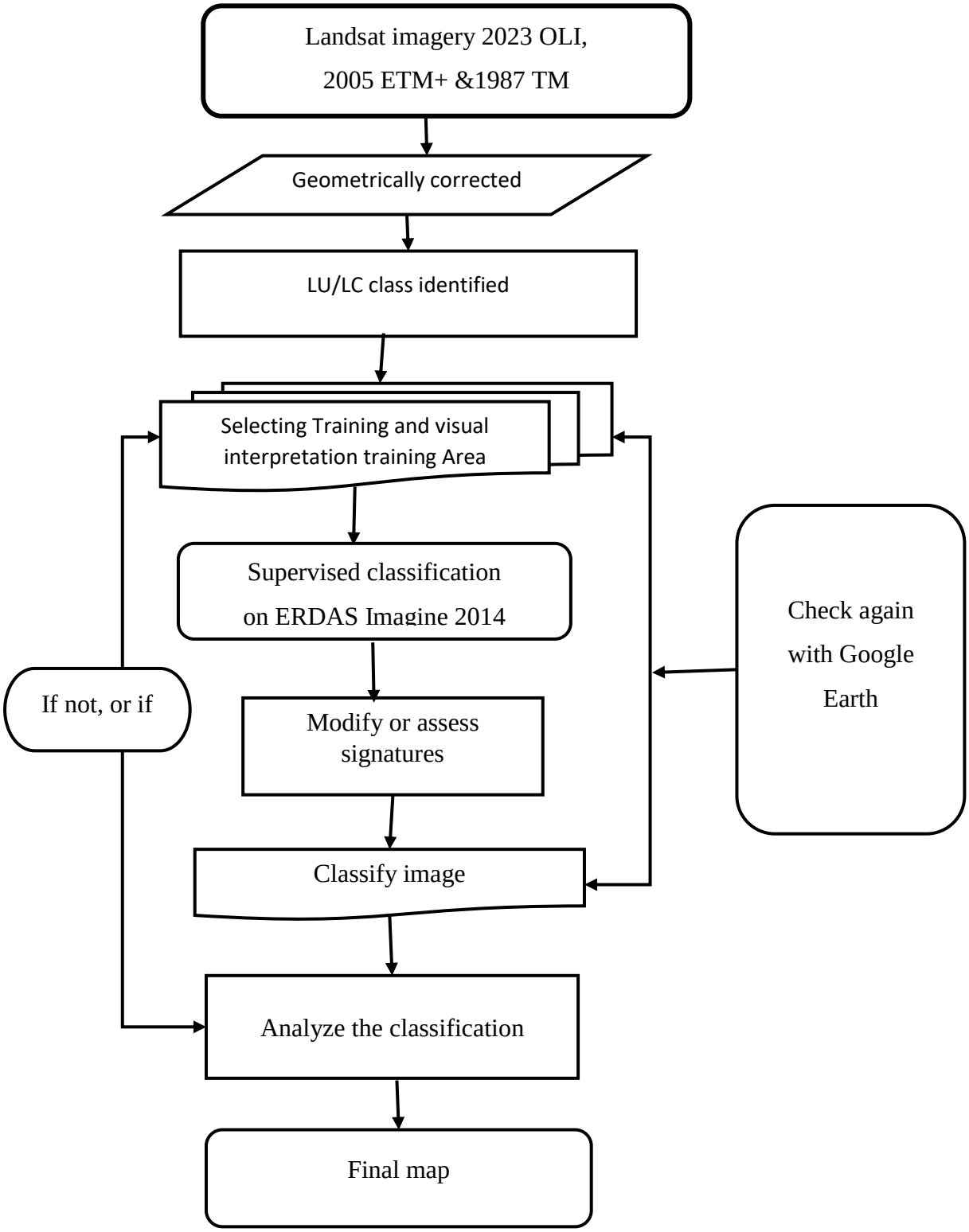

Figure 3. 9: Methods and techniques used to categorize land cover and usage from a Landsat image.

3.4. Land-use/cover change detection

In Asella and its surrounding areas, situated in a developing nation, a significant alteration in LC/LU was observed due to both natural phenomena and human activities. The process of change detection, which involves identifying changes in specific areas, was initiated. Many remote sensing projects undertook the evaluation of images captured at different points in time to gauge the extent and nature of changes over time. Among the widely adopted approaches for change detection purposes was post-classification. The task involved analyzing land-use/land-cover change by utilizing images from 1987, 2005, and 2023.

To analyze LU/CC maps, technical procedures of integration utilizing ArcGIS software techniques were employed. The initial step entailed developing a table that indicated the area coverage in square kilometers and the percentage change for each year (1987, 2005, and 2023) measured against each LU/LC class. Thus, to calculate the LU/CC in percentage, the equation was utilized. Therefore, to calculate LU/CC in percentage equation (eq.3.1) was used (Lambin et al, 2001).

$$\text{Percentage change} = \frac{\text{Observed change}}{\textit{Some of Area}} \times 100 \quad \text{.....Eq. (3.1)}$$

3.5. Normalized difference vegetation index and LSTderivation

3.5.1. Normalized difference vegetation index estimation

Among the most widely utilized urban climate indicators in environmental studies is the NDVI, which serves as a reliable index for extracting vegetation conditions from remotely sensed data. NDVI is a crucial component of LST estimation since it is directly utilized to calculate land surface emissivity. (Guha & Govil, 2020). The NDVI has values ranging between −1 and +1, where negative values indicate non-vegetated areas and positive values represent vegetated areas. The NDVI of the study area was extracted using Equation (3.2).

$$\text{NDVI} = \frac{\text{NIR(Band 4,5)} - \text{RED (Band 3,4)}}{\text{NIR(Band 4,5)} + \text{RED (Band 3,4)}} \quad \text{..... Eq. (3.2)}$$

The NDVI is computed using Equation (3.2), where NIR denotes near-infrared band 4 and R denotes red band 3. Several sensors, including OLI for 2023, ETM+ for 2005, and TM for 1987, were calculated using this formula. However, Weng et al. (2004) Observe that there is a significant discrepancy in Landsat 8 band identification, with the red band corresponding to band 4 and NIR to band 5.

In addition to the NDVI, fractional vegetation cover (FVC) was also calculated using equation (3.3). This formula provides a means of quantifying the amount of vegetation found in a given area, which contributes to the understanding of ecosystem dynamics and land use patterns. This study uses the same methodologies across different sensors and accounts for band changes to guarantee the validity and consistency of vegetation-related measures over time and across multiple satellite platforms.

$$FVC = \frac{NDVI - NDVI_S}{NDVI_v - NDVI_S} \quad \text{Eq. (3.3)}$$

Where,

FVC=Fractional Vegetation cover

The above equation (FVC) was used to get a fraction of an area with vegetation cover using the NDVI value.

$\mathrm{NDVI_s} = \text{IS NDVI for soil and } \mathrm{NDVI_V} = \text{NDVI for vegetation}$

3.5.2. Land Surface Temperature Retrieval

To compute LST and collect accurate temperature readings for a specific study period, a variety of different processes need to be performed. This study used thermal bands from Landsat imagery, which includes the Landsat 5, Landsat 7, and Landsat 8 satellites, to calculate LST values for the years 1987, 2005, and 2023. More specifically, the entire temporal spectrum was covered by using Thermal Infrared (TIRS) bands 6 for Landsat 5 and Landsat 7, and Thermal Infrared (TIRS) 1 and 2 for Landsat 8.

The LST calculation methodology was in line with earlier research approaches used by researchers like (Imran et al., 2021) and (Kafy et al., 2020) This involved using the mono-window algorithm and split-window technique a reliable computational technique that is well-known for its effectiveness in obtaining LST values from thermal infrared images. This investigation aims to advance a more comprehensive comprehension of LST dynamics by following established protocols and utilizing advances in remote sensing technology. This enabled informed decision-making in a variety of fields, including land management and climate science.

3.5.3.Radiometric correction

In remote sensing, radiometric correction is the action of converting digital numbers into spectral radiance values, which is essential for precise data processing. According to (Prata et al., 1995),

this correction method consists of a set of image-processing steps that are intended to correct flaws that are present in the raw data. One of these processes involves converting digital number (DN) values to radiance and then transforming those values into reflectance values. This process improves the accuracy and consistency of the obtained images.

The mathematical foundation for converting digital representations of electromagnetic energy recorded by remote sensors into quantifiable radiance values throughout the electromagnetic spectrum is provided by this equation. Practitioners guarantee radiometric correction procedures' accuracy by following protocols like this one. This makes it easier to read and analyze remote sensing data more accurately for various applications ranging from urban planning to environmental monitoring.

Equation (3.4) is used to convert digital integers to spectral radiance, following the methodology's instructions.

$$L_\lambda = L_{Min} + (L_{Max} - L_{Min}) \times DN/255 \quad \text{.....Eq. (3.4)}$$

Where,

L_λ= spectral radiance

L_{Min}=minimum radiance

L_{Max}=maximum radiance

DN=digital number value of the pixel

3.5.4. At sensor spectral radiance, conversion

The process for creating LST from thermal bands commenced with the conversion of DN to Spectral Radiance. The DN of thermal infrared (TIR) bands were transformed into spectral radiance using the Radiative Transfer Equation (RTE) presented in Equations.

Whereas for Landsat OLI/TIRS, Equation (3.5). For Landsat TM, spectral radiance L_λ

$$L_\lambda = \frac{L_{Max_\lambda} - L_{Max_\lambda}}{Q_{Cal_{Max}} - Q_{Cal_{Max}}} * Q_{Cal_{Maxl}} - Q_{Cal_{Min}} + L_{Min_\lambda} \text{..... Eq. (3.5)}$$

Was utilized L_λ is the spectral radiance value; Q_{Cal} symbolizes the quantized calibrated pixel's DN value.. L_{Max_λ} shows the spectral radiance value in $W_M{-^2}_{Sr}{-^1}_{\mu m}{-^1}$ scaled to;$L_{Min\,\lambda}$ shows the spectral radiance value in $W_M{-^2}_{Sr}{-^1}_{\mu m}{-^1}$ scaled to $Q_{Cal_{Min}}$ and $Q_{Cal_{Max}}$ are the min and max DN values of the quantized calibrated pixels that correspond to $L_{Min\,\lambda}$ and L_{Max_λ} respectively was computed using Equation (3.6)

$$L_\lambda = M_L \times Q_{Cal+A_l} \quad \text{..... Eq. (3.6)}$$

Where L_λ represents the TOA spectral radiance in ($W_M{}^{-2}{}_{Sr}{}^{-1}{}_{\mu m}{}^{-1}$)

ML is the rescaling factor for the radiance multiplicative band obtained from metadata

Qcal is the DN is the value of the calibrated and quantized product pixel.

AL is the rescaling factor for the radiance additive band obtained from metadata.

3.5.5. Radiance to BT conversion

Thermal infrared data can undergo conversion from atmospheric reflectance (L_λ) to effective sensor brightness temperature *B*T utilizing thermal constants provided in the metadata file. Specifically, for the Landsat OLI/TIRS thermal band, which corresponds to band 6 on thematic mapper and enhanced thematic mapper plus, conversion is required from at-sensor spectral radiance to effective at-sensor brightness temperature. Subsequently, brightness temperature represents the radiance ascending from the summit of the earth's atmosphere. To compute the brightness temperature values at the TOA, equation (3.7) as outlined by Rajeshwari and Mani (2014) was employed.

$$BT = \frac{K_2}{\ln(\frac{K_1}{L_\lambda} + 1)} \quad \text{..... Eq. (3.7)}$$

Effective at satellite brightness temperature (unit in Kelvin)

K2=calibration constant 2

Ln=natural logarithm

K1=calibration constant 1

Landsat 8 has two thermal bands (Radiance add bands 10 and 11). Table 3.7 shows the calibration constant used while performing the formula for brightness temperature.

Table 3. 7: Thermal band calibration constant of Landsat 8.

Satellite & sensors	Categories	Band 10	Band 11
Landsat 8 OLI/TIRS	K1	777.8853	480.8883
	K2	1321.0789	1202.1442
	Radiance MULT_BAND	0.0003342	0.0003342
	Radiance ADD_BAND	0.01	0.01

The calibration constant for Landsat 5 and Landsat 7 is different from Landsat 8. In the case of Landsat 5 and Landsat 7 the following table 3.8 was used.

Table 3.8: ETM+ and TM thermal band calibration constant.

Satellite	sensors	constant	value
Landsat 5	TM	K1	607.75
		K2	1260.55
Landsat 7	ETM+	K1	666.1
		K2	1282.7

3.5.6. Derivation of LST from BT

Equation (3.8) was then used to calculate the LST from BT. The at-satellite brightness temperature at this point was used to calculate the corrected LST (in Kelvin).

$$\mathrm{LST}(^{\circ}\mathrm{K}) = \frac{\mathrm{B_T}}{[1 + \lambda\left(\frac{\mathrm{B_T}}{\mathrm{E}}\right)\ln(\varepsilon)]} \quad \text{..... Eq. (3.8)}$$

Where BT is the brightness temperature at-satellite (sensor); λ is the wavelength of emitted radiance (i.e., 11.5 μm in Band 6 for Landsat 4/5/7 and 10.8 μm in Band 10 for Landsat 8); E is (h × v)/s (1.4388×10^{-2}mK); h represents the Planck's constant (6.626×10^{-34}mK); v represents the velocity of light (2.998×10^{8} m/s). Represents the Boltzmann constant (1.38×10^{-23} JK), and ε represents the emissivity of the land surface.

Equation (3.9) was then used to compute the ε, which involved utilizing Equation (3.10) to get the vegetation proportion (Pv)

$$(\varepsilon) = N\,(Pv) + n \quad \text{..... Eq. (3.9)}$$

Where N is a constant (0.004).

n is a constant (0.986).

Pv is the vegetation proportion, which is calculated based on the NDVI values.

The NDVI values are scaled by this equation from 0 to 1, which represents the percentage of vegetation cover. A higher percentage of vegetation cover is indicated by higher Pv values, whereas lower values imply a smaller proportion of vegetation cover in Equation (3.10).

$$P_v = \left(\frac{NDVI - NDVI_{min}}{NDVI_{max} - NDVI_{min}}\right)^2 \quad \text{....... ....Eq. (3.10)}$$

Where NDVI are the values of DN obtained from the NDVI image; NDVI max and NDVI min are the highest and lowest DN values obtained from the NDVI image. Lastly, the land surface temperature value (in Kelvin) was converted into degrees Celsius (◦C) using the last equation (3.11).

LST (◦C) = LST (◦K) − 273.15 ....Eq. (3.11)

Where:

◦C is the Land Surface Temperature in Celsius.

◦Kis the Land Surface Temperature in Kelvin.

For sensors like TM and ETM+, the LST is often computed by deducting 273.15 from the temperature obtained using the satellite's effective temperature formula, expressed in Kelvin.

3.6.Validation of estimated LST

To guarantee the precision and dependability of the data for the purposes for which it was intended, estimated LST validation is essential. One important step in determining how well the obtained LST values match the intended activity is verification. Random sample locations covering a range of land cover types and conditions were chosen from Google Earth for this validation process. The Landsat 8 TIRS was utilized to obtain LST imagery and zonal statistics were employed to retrieve the LST values associated with these sites. Finally, by comparing the mean LST values of each polygon, a comprehensive evaluation of the precision and consistency of the calculated LST in diverse spatial settings was made possible.

The validation process ensures the robustness of assessing the correctness of the estimated LST by utilizing a systematic methodology that combines zonal statistics, random sampling, and comparative analysis. This approach detects and corrects possible inconsistencies or errors in the LST estimation, thereby enhancing the data's reliability for additional research and decision-making procedures. All things considered, confirming that the data is appropriate and valuable for the intended uses is made possible by validating the estimated LST is a crucial step in the quality assurance process.

3.7. Zonal analysis

Statistical analysis is essential for examining various variables, including both dependent and independent ones. In this study, statistical methods were employed to investigate the correlation between LU/LC and LST. Correlation analysis was utilized to explore, how LST and NDVI are related. This analysis involved converting the pixels within the reflectance value.

Additionally, any area in the input that has the same value is known as a zone. Condensing a raster's values inside the boundaries established by another dataset—raster or vector—is accomplished by the Zonal Statistics function, which then displays the results in tabular form. For the years 1987, 2005, and 2023, maps showing LU/CC, NDVI, and LST were created. To examine the spatial variation of LST about various LU/LC changes, the data were combined using ArcGIS 10.8's Zonal Statistics tool. The LU/CC, NDVI, and LST map summarized data were then examined using Microsoft Excel. Table-based zonal statistics is a vital tool used to investigate the relationship between LU/LC and LST.

CHAPTER FOUR

ANALYSIS AND PRESENTATION

4.1. Accuracy assessment

The LU/LC accuracy assessment revealed that the total categorization accuracy for the years 1987, 2005, and 2023 was 85.66%, 87.33%, and 89.95%, respectively. The Kappa statistics classification for 1987 was 0.80, while the corresponding Kappa values for 2005 and 2023 were 0.80 and 0.81, respectively. The detailed information on producers' and users' accuracy is indicated in Table 4.1.

Table 4 1. Statistical information of accuracy assessment for 1987, 2005, and 2023.

Class	1987		2005		2023	
	producers accuracy	users accuracy	producers accuracy	Users accuracy	producers accuracy	users accuracy
Forest	0.857143	0.75	0.962963	0.787879	0.791667	1
Shrub land	0.8	0.682927	0.684211	0.896552	0.625	0.714286
Farmland	0.856322	0.955128	0.94375	0.89881	0.957055	0.934132
Settlement	0.909091	0.76191	1	0.6	1	0.81818
Waterbody	1	0.9375	0.95	1	1	1
Bare land	0.840909	0.880952	0.651163	0.903226	0.5625	0.75
Overall classification accuracy	**85.66%**		**87.33%**		**89.95%**	
Kappa statistics	**80.08**		**80.73**		**81.33**	

4.2. Land-use/ cover-change in 1987, 2005 and 2023

The land-use/land-cover classification of 1987 showed that the main LU/LC classes were farmland and shrubland. These classes accounted for 677.27 km², (70.47%) of the overall area coverage. From the total area of 961.01 km², farmland accounted for 512.24 km², (53.3%) and shrubland accounted for 165.02 km², (17.2%). The other LU/LC, bare land, forest, settlement, and water bodies accounted for 283.74 km², (29.53%) of the total area. Of all the classes, the settlement

covered 47.72 km², (4.96%) was the smallest. Analysis of the 2005 image also revealed that, at 560.36 km², (58.41%), the cultivated area makes up the majority of the land in the study region, with bare land (10.33%) and forests (10.8%) coming in second and third. Shrubland, settlement, and water bodies were the other LU/LC groups comprising 20.53% of the total area. The smallest area was occupied by settlements (5.45%) and water bodies (5.42%) in 2005 compared with all other classes. According to the LU/LC classification results of 2023, farming accounted for 653.27 km² (67.94%) of the entire coverage area, making it the leading LU/LC class category. People occupied 80.58 km² (8.38%). Bare terrain, forests, shrublands, and water bodies comprised the remaining LU/LC classes, making up 23.68% of the total area. Nonetheless, farmland expanded from 53.3% in 1987 to 67.9% in 2023. Farmland is typically the largest LU/LC in terms of area coverage. Table 4.2 displays a comprehensive statistical summary of each class, the LU/LC classes, and area coverage over the study period.

Table 4 2. Shows a summary of LU/LC classifications together with net changes for Asella and its surrounding area in 1987, 2005, and 2023.

LU/LC classes	**1987**	**2005**	**2023**	**The net change from 1987 to 2023**
	Area (km²)	**Area (km²)**	**Area (km²)**	**Area (km²)**
Farmland	512.2423	560.3634	653.2660	141.02
Bare land	112.4623	99.0222	43.3131	-69.15
Forest	72.0481	103.6204	74.5614	2.512
Settlement	47.7257	53.3558	80.5853	32.86
Waterbody	51.5109	53.0325	55.8126	4.35
Shrub land	165.0253	91.8433	53.9456	-111.12

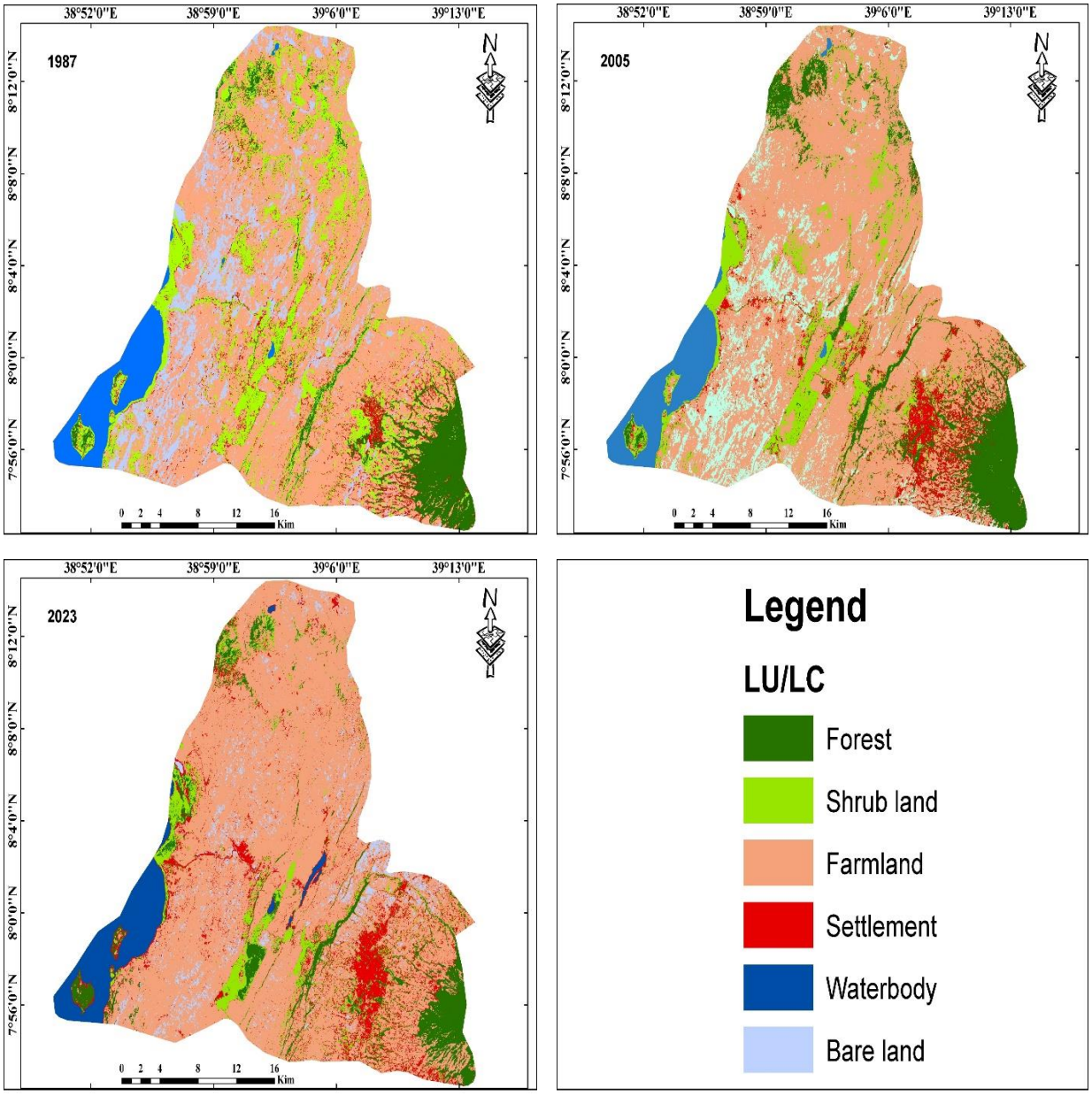

Figure 4. 1. Maps showing the land cover and use in the research areas from 1987 to 2023.

The LU/LC changing trends within the research domain showed a notable decline in bare land and shrubland. Bare land shrank from 112.462 km² (11.7%) to 43.313 km² (4.5%), while shrubland decreased from 165.025 km² (17.17%) to 53.945 km² (5.6%). Conversely, though, the area coverage of the other LU units varied in different degrees. Figure 4.2 shows the pattern of the changes.

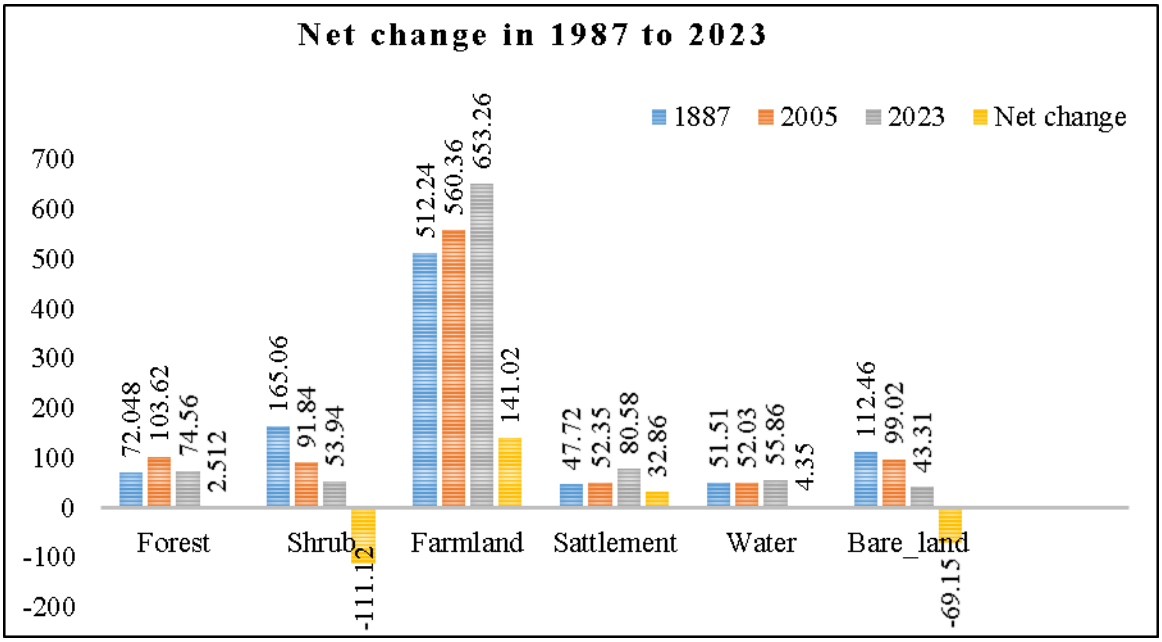

Figure 4. 2. Shows the distribution, changes in LU/LC patterns, and together with net changes of the research area from 1987 to 2023.

4.3. The geographical range of LU/LC

LU/CC patterns in the study area indicate a significant change between 1987 and 2023. Among the six major LU/LC classes, Over 53% of the study region was covered by farms overall study years. Farmland increased from 53.302% in 1987 to 58.417% by 2005 and increased to 67.939% in 2023 because of the substantial rise in agricultural land between 1987 and 2023 can be ascribed to various factors such as population growth, economic incentives, technical developments, and government policies that support the spread of agriculture. In addition, a variety of terrain types have been converted to farms due to reasons like deforestation, climate change, global market demand, and sociocultural values. The development of reservoirs and ponds to support increased agriculture, along with improved irrigation techniques, are the main causes of the growth in water bodies from 5.360% in 1987 to 5.809% in 2023, particularly with the addition of additional water features in the map's center regions. Additionally, by modifying precipitation patterns and raising runoff, natural hydrological changes and climate change have contributed to this expansion. The extent of bare land decreased between 1987 and 2023. It decreased from 11.702% in 1987, 10.323% in 2005, and 4.504% in 2023. The settlement area has been increasing from 1987 to 2023. It increased from 4.966% in 1987 to 5.458% in 2005 and 8.381% in 2023. Shrub land decreased

from 1987 to 2023. It decreased from 17.172% in 1987, 9.574% in 2005, and 5.610375 % in 2023. Forest showed fluctuations from 1987 to 2023. Forest was 7.497% in 1987, which increased to 10.802% in 2005 and then decreased to 7.754% in 2023. The net changes information in (Table 4.1)

The LU/LC change trends within the research domain indicated a 69.15 km² decrease in bare land and a 111.12 km² decrease in shrubland. The area covered by forests varies. The area increased by 2.512 km² between 1987 and 2023. A growing 178.23 km² area coverage was seen in other classes.

4.3. Settlement expansion during 1987–2023

One of the other temperature factors in urban regions is higher than in rural areas. Cities can reduce urban heat island effects (UHIs) by using cool, reflective materials for pavement and roofing planting trees and green roofs, and improving urban planning to encourage compact growth and improve airflow. A city can be a source of heat due to various factors. Among the physical factors, the reflection of sheet metal, the reflection of asphalt, the color of buildings, and other factors can increase the temperature in urban areas.

An overlay analysis of settlement area detected from 1987, 2005, and 2023 satellite images of Asella and its surrounding area revealed that the farmland, shrubland, and bare land had been changed to settlement areas in different directions of the study area. The spread of the settlement area towards other LU/LC classes is shown in Figure 4.3.

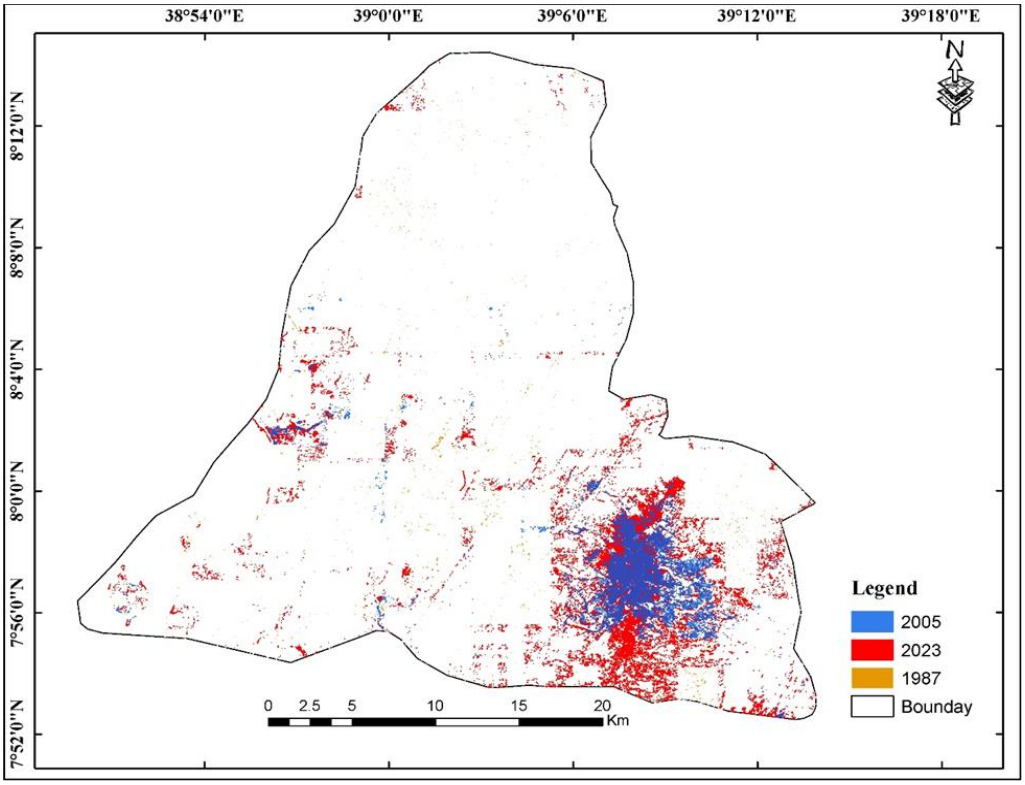

Figure 4. 3. The pattern of the settlement area's growth from 1987 to 2023

4.5. Normalized difference vegetation index

In this study, vegetation cover was higher in 1987 and 2005, with maximum NDVI values of 0.519 and 0.461, respectively. The forest area cover was below 10.8%, contributing to the NDVI values exceeding 0.519. Vegetation is healthy when its value is highest. Vegetation cover decreased for 2023 with an NDVI value of 0.375.

The southeastern regions of the research area had higher NDVI values, according to the NDVI data of 1985, 2005, and 2023. The Intoto Mountain, which is covered in a forest, had the highest NDVI value. Nonetheless, the NDVI values are comparatively low in the southwest, Waterbody locations along the Ziway region. Throughout the study, non-vegetated areas have gradually increased while vegetation cover has gradually declined, as shown in Figure 4.4. However, in 2023, the Shurb land area slightly decreased because of the expansion of farmland.

Table 4. 1. Statistical information on NDVI values for 1987, 2005, and 2023.

Year	Min	Max	Mean	Std.Deviation
1987	-0.15	0.52	0.12	0.08
2005	-0.15	0.46	0.10	0.06
2023	-0.11	0.38	0.10	0.04

According to the study, the greatest NDVI values of 0.519 and 0.461, respectively, in 1987 and 2005, indicated the highest levels of vegetation cover, indicating healthier vegetation. But by 2023, there was a noticeable decline in vegetation, as the NDVI fell to 0.375. In 1985, 2005, and 2023, the study area's southeast regions continuously displayed higher NDVI values; the Intoto mountain forested area had the highest values. Conversely, the water body locations in the southwest along the Ziway region showed relatively lower NDVI values. Figure 4.4 shows that over the study period, there was a drop in plant cover and an increase in non-vegetated regions. However, the increase in farming in 2023 resulted in a modest decrease in the shrubland's extent. The statistical breakdown of the NDVI values for 1987, 2005, and 2023 is given in Table 4.4.

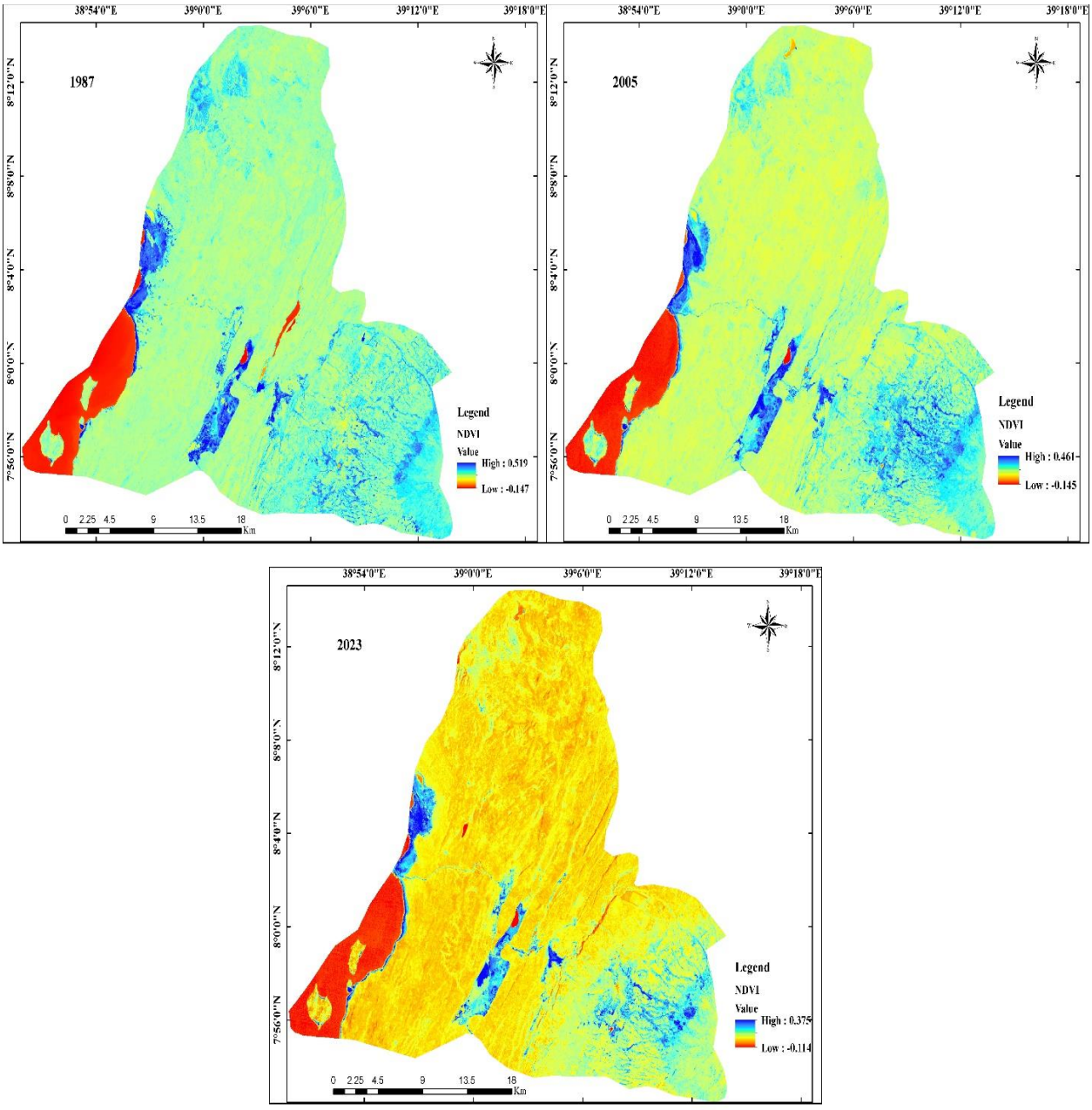

Figure 4. 4. Study maps normalized differential vegetation index (1987, 2005, and 2023).

4.6. Land use/Land cover and the NDVI relationship

Using the near-infrared and red bands of the research periods as a source, NDVI maps revealed that the NDVI values of various LU/CC varied. The NDVI value fluctuates from area to area depending on the site's intensity of vegetation because it is correlated with vegetation conditions. Forest and shrubland have the highest NDVI value than other classes (Fig. 4.5).

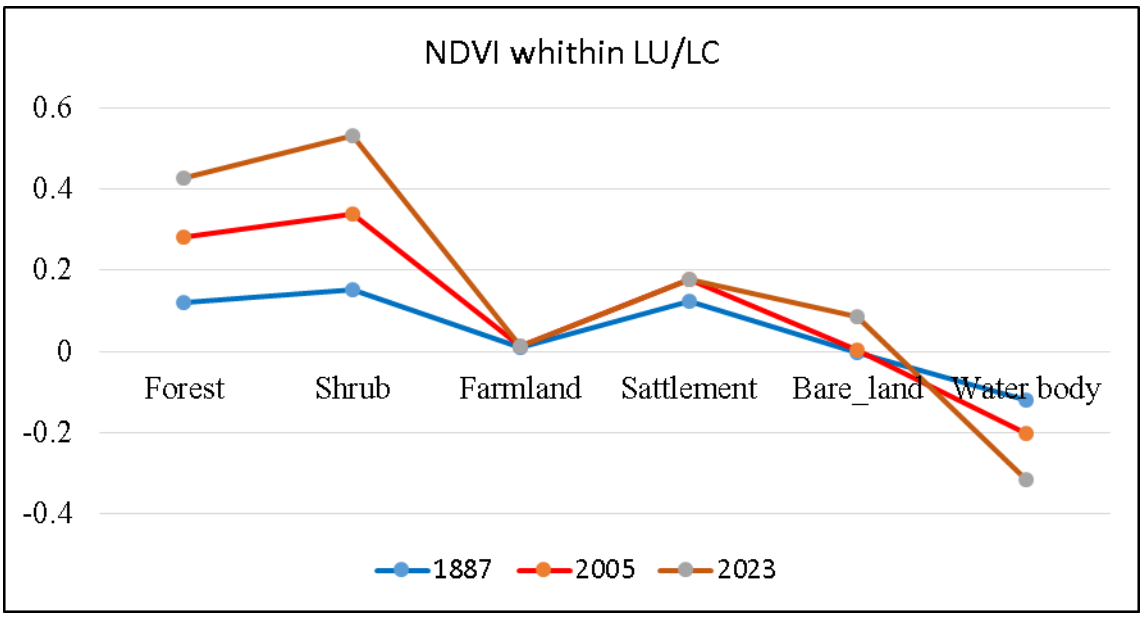

Figure 4. 5. Zonal statistical depiction of the NDVI for the study area's various LU/LC classes in 1987, 2005, and 2023.

4.7. The LST spatial pattern in Asella and its surrounding areas.

Using Landsat TM from 1987, ETM+ from 2005, and 2023 for OLI/TIRS thermal bands, the spatial distribution of LST of the research area was retrieved and quantified. As observed in the processed thermal images, the research period's LST value varied between 8.74°C and 48.85°C. The analyzed thermal images revealed that the northeast, central parts of the study, and part of the northern areas showed comparatively high temperatures. The primary causes of this include LU/LC kinds, slope, and altitude. However, the southern and southeastern regions, including the highlands of the Chillalo Mountain range, exhibited lower LST values due to their higher altitudes, ranging from 3095 to 3868 meters above sea level (a.s.l.). The elevation and vegetation cover in these regions played crucial roles in mitigating heat absorption and enhancing cooling effects. Similarly, the southwestern regions near Ziway water bodies, with altitudes from 1620 to 1881 meters a.s.l., also showed lower LST values. Understanding the spatial and temporal dynamics of LST is essential for effective land management and urban planning, with targeted interventions such as increasing green cover, implementing sustainable agricultural practices, and promoting urban green spaces necessary to mitigate rising temperatures. Continuous monitoring using remote sensing data and exploring the relationship between LST and other climatic variables, like precipitation and humidity, will enhance the overall resilience of the region to climate variability.

The presence of water bodies significantly influences the microclimate by providing a cooling effect and regulating temperature fluctuations. For each period, the LST distribution is shown in Figure 4.6.

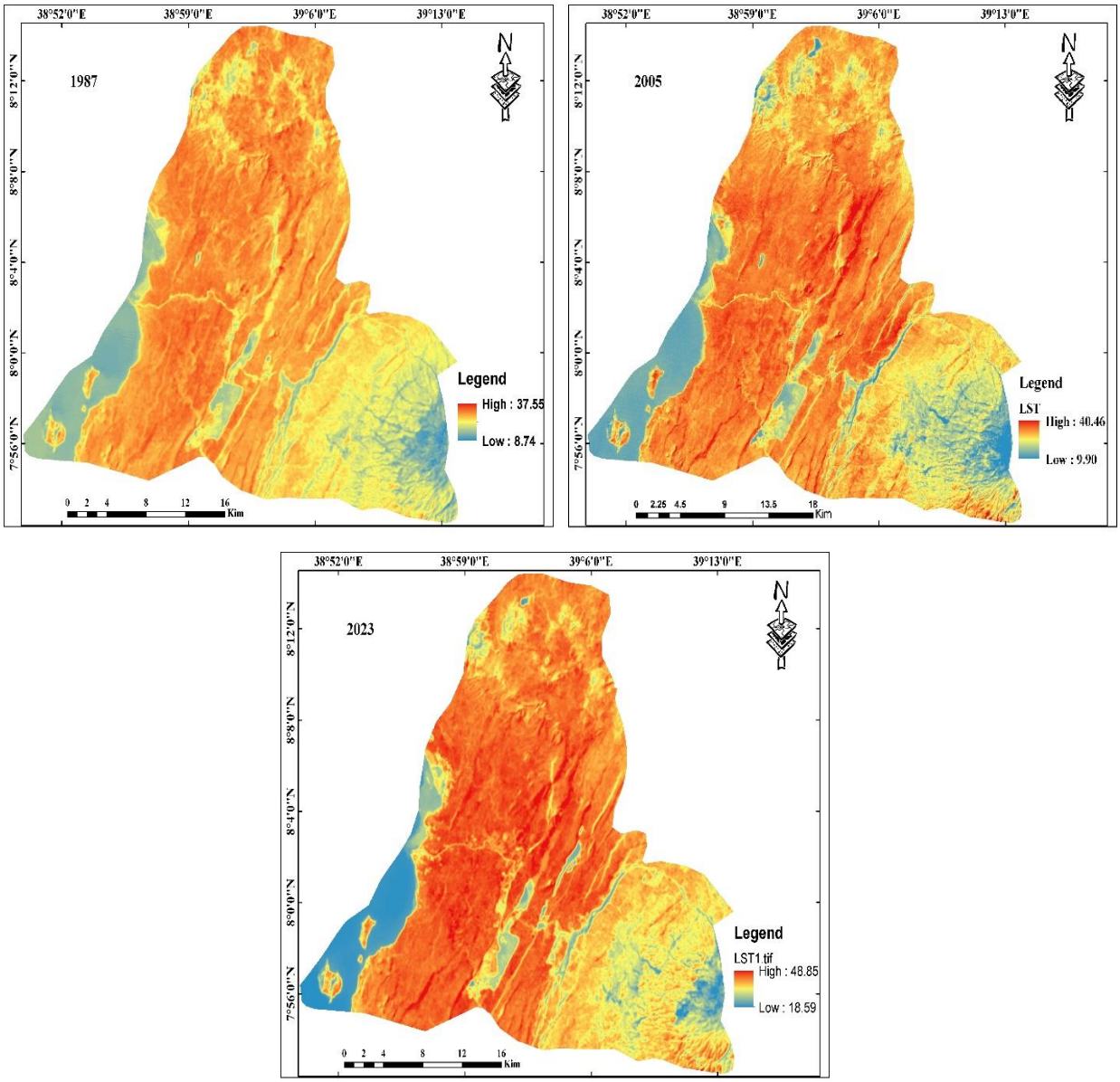

Figure 4. 6. Land surface temperature maps of the study area from 1987, 2005, and 2023

4.8. Changes in LU/LC and their effects on LST

The dynamics of LU/LC impact surface temperature. The LU/LC oscillations caused changes in the LST, particularly in bare terrain areas, cultivation (after harvest), and settlement. Due to the dry weather and harvest season when the image used for the investigation was taken, farmland LU/LC classes had high LST because of harvesting often moderates soil moisture content because crops no longer draw water from the soil through their roots, resulting in less transpiration. Dry soils heat more quickly than moist soils because water has a high heat capacity and helps to moderate temperature fluctuations. Due to regional differences in vegetation and climate, the LST value varies for each LU/LC class. The LST increased because farming and other land uses were converted into settlement areas. The settlement area has significantly expanded, as shown in Figure 4.4 (Expansion of Settlement Area from the Year 1987 to 2023), particularly in the northern and southern portions of Asella and its surrounding areas along the main town gate (Adama, Iteya, Sagure, and Bekoji). Furthermore, the research region's minor towns have seen a growth in the Dugda town area.

Table 4. 2. LST's zonal statistical description across various LU/LC in 1987, 2005, and 2023

LU/LC classes	1987				2005				2023			
	Min	Max	Mean	Std	Min	Max	Mean	Std	Min	Max	Mean	Std
Forest	8.73	31.7	17.62	3.82	9.89	39.5	21.68	4.39	18.5	46.9	28.91	4.52
Shrub land	10.15	36.01	24.62	4.612	13.27	40.01	26.88	4.265	19.51	45.16	31.91	4.033
Farmland	11.09	37.54	28.05	3.33	14.92	40.45	29.17	2.64	21.7	48.85	38.84	3.23
Settlement	9.68	36.01	20.47	3.61	12.71	39.11	24.48	3.58	19.25	48.26	34.23	4.28
Waterbody	12.49	23.1	14.64	1.09	13.82	23.85	16.97	0.61	19.24	33.27	20.67	1.47
Bare land	18.79	36.77	29.93	2.17	17.62	40.01	31.51	1.79	25.9	47.44	39.06	2.5

where Std is the standard deviation, Max is the maximum, and Min is the minimum.

During the study period, over 53% of the study area was covered by cropland. From a mean temperature of 28.05ºC in 1987 to 38.84ºC in 2023, the LST value has grown. The Bare land and Shrub land also impact of LU/LC changes on LST variability is seen in Figure 4.8.

4.9. Relationship between LST and land use/cover

The study area's land-use/cover and LST maps showed how the categories and associated land-surface temperatures evolved throughout the investigation. The LU/LC types with the lowest temperatures were shrubland, forest, and water bodies, in that order. The presence of vegetation and water bodies played a crucial role in reducing the LST.

Different sections of the area with vegetation and trees create shade, which lowers LST through evapotranspiration—the process by which plants release water into the surrounding air. The areas with the greatest LST values were barren terrain, agricultural, and settlement. During the time the image was being acquired, the LST value was high in agricultural areas. The average LST of Asella and its surrounding areas raised the temperature of farmland by 32.02°C between 1987 and 2023. According to Table 4.5, the LST has increased for every major LU/LC category during the study. Farmland, bare land, and populated areas had the greatest mean LST values. Conversely, places with shrublands, woods, and bodies of water had the lowest mean LST. Between 1987, 2005, and 2023, there was a discernible rise in the research area's mean temperature. The average temperature of the forest was 17.64°C in 1987, rising to 21.69°C in 2005 and then reaching 28.97°C by 2023. The overall change in temperature from 1987 to 2023 indicates a large climb, and this increasing trend reveals severe warming in the region. The information emphasizes how the land surface temperature in the research region is impacted by elements including urbanization, deforestation, and climate change. Figure 4.7 shows comparisons of the study periods' mean LST with LU/LC classes.

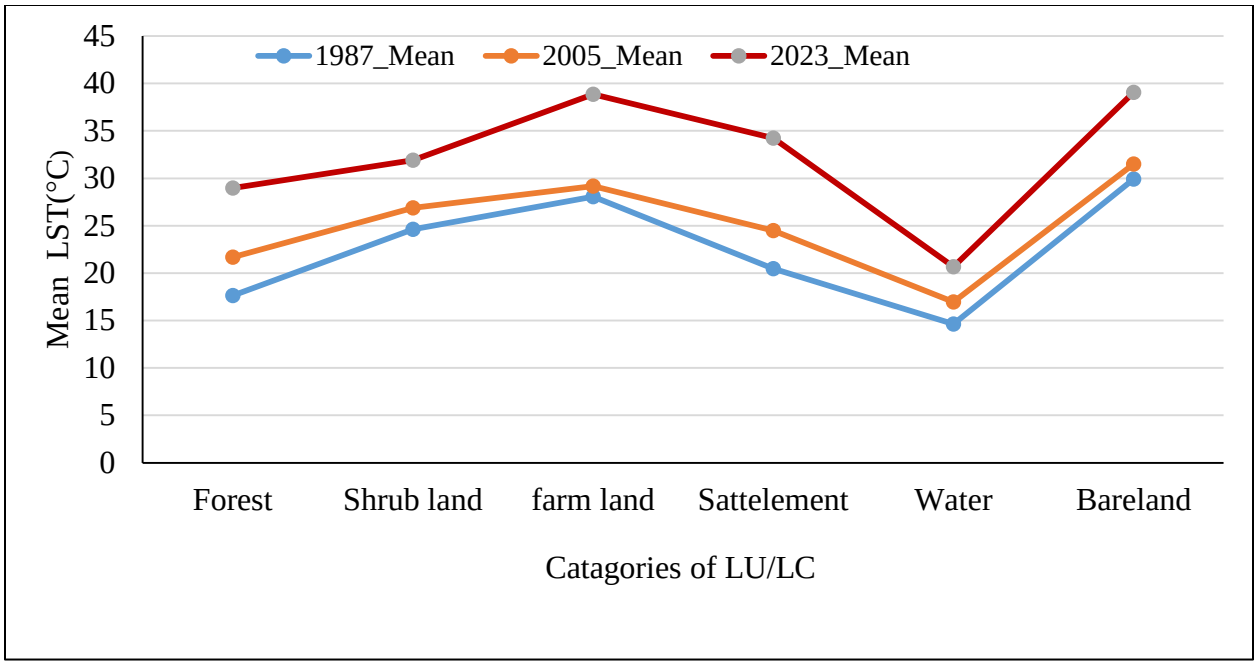

Figure 4. 7. Compares the mean LST of Asella and its surrounding areas of the investigation across multiple LU/LC groups.

Table 4. 3. Mean temperature of 1987, 2005, and 2023 and changes in temperature during 1987-2023 in the study area

LU/LC Classes	1987_Mean	2005_Mean	2023_Mean	1987_2005 Change in (ºC)	2005_2023 Change in (ºC)	1987–2023 Change in (ºC)
Forest	17.64469	21.69304	28.97712	4.048348	7.284079	11.332427
Scrub land	24.62883	26.88486	31.91966	2.256033	5.034803	7.290836
Farmland	28.05472	29.17803	38.84968	1.123308	9.671651	10.794959
Settlement	20.47706	24.48533	34.23337	4.008275	9.748036	13.756311
Water	14.64783	16.97605	20.67702	2.328221	3.700969	6.02919
Bare land	29.93328	31.51896	39.0632	1.585681	9.129918	10.715599

Deforestation and various global impacts are affecting all land cover with increasing global temperatures. Measuring the summertime temperatures of exposed soil, cut grass, and uncut grass is a straightforward experiment with a powerful lesson. Although The outcomes are self-evident,

including a reading from the hedge would have been fascinating. The impact of LU/CC on LST variability is seen in Figure 4.8.

Figure 4. 8. Contrasting views on the land surface temperature in the research area in 2023.

4.10. Relationship between land surface temperature and the NDVI

There are indirect correlations between NDVI and LST, according to an analysis of Landsat data from 1987, 2005, and 2023. High NDVI values have low LST, while low NDVI values have high LST. Nonetheless, given that the water body had lower NDVI and LST values, there was a direct and positive association between the two variables in this instance. On the other hand, low NDVI values, which represent scant vegetation, are linked to higher LST because they result from less shade and evapotranspiration as well as increased solar energy absorption and reradiation by bare surfaces. On the other hand, the situation with water bodies is different. Because water bodies reflect less near-infrared light than vegetated regions, they usually have lower NDVI values. Water bodies have a high specific heat capacity, which enables them to absorb and hold heat without experiencing appreciable temperature changes while having low NDVI values. This helps water bodies maintain lower LST. As a result, there is a clear and positive correlation between NDVI and LST when it comes to water bodies. In contrast to vegetated or bare ground, water bodies exhibit lower LST even at low NDVI. The inherent thermal characteristics of water, which are essentially different from those of terrestrial surfaces, are the cause of this anomaly. During the study period, the R^2 values for the NDVI and LST were 95.43%, 96.52%, and 95.57%, respectively. In 1987; 2005; and 2023. These findings demonstrate that the NDVI value difference

was responsible for the year 1987 is 95.43% of the LST due to the difference in NDVI value, the coefficient variation values are also the same for 2023. In general, a negative association between NDVI values and LST was discovered. Figure 4.9 displays the LST and NDVI connection for the years 1987, 2005, and 2023.

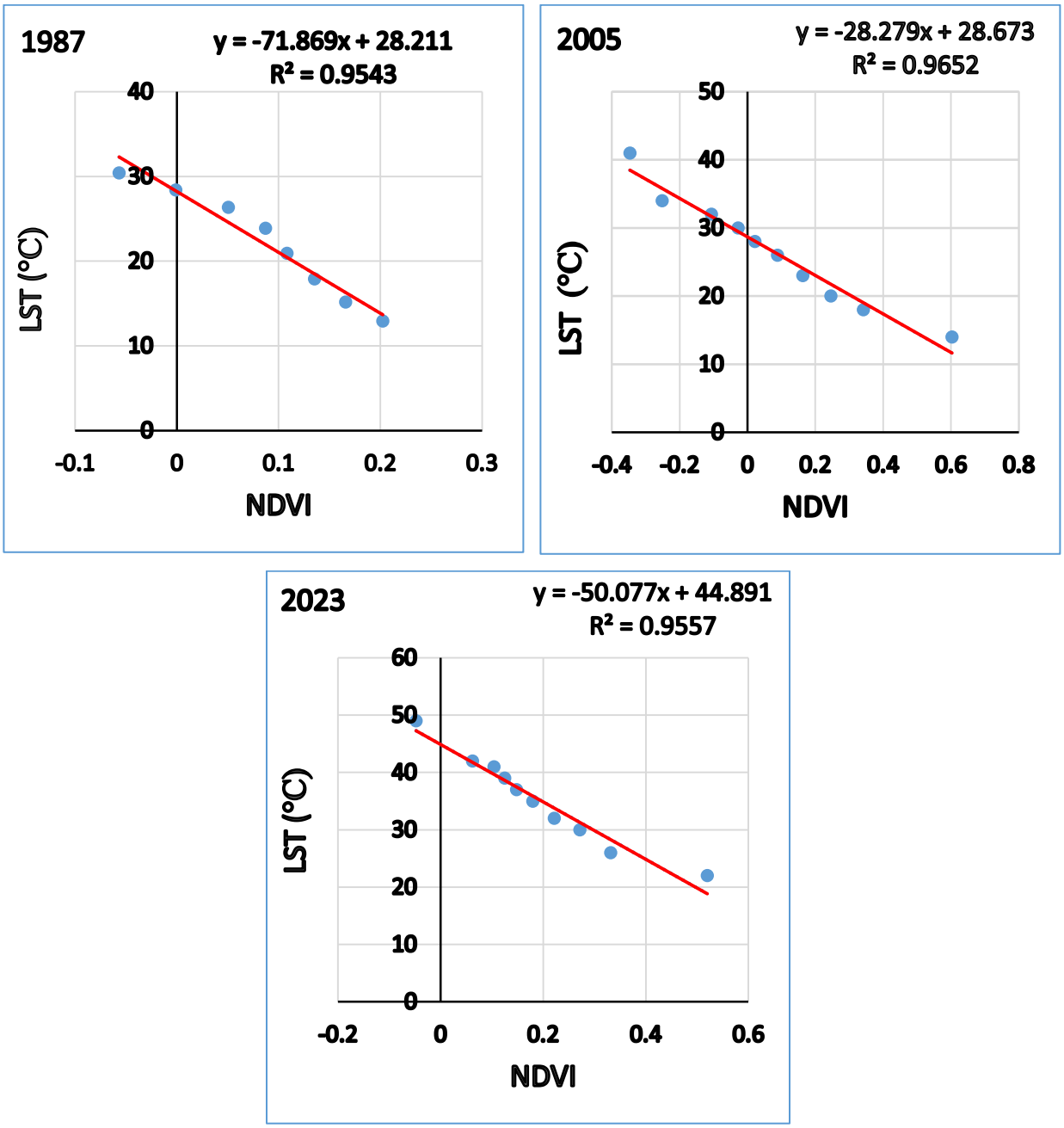

Figure 4. 9. Land surface temperature and NDVI correlation for the years 1987, 2005, and 2023 for the study area.

4.11. Comparisons of LST distribution during 1987, 2005, and 2023

The study's findings showed that the LST value rapidly increased throughout the investigation. Six groups of land surface temperatures, ranging from 8.74 ºC to 48.85 ºC, were created. Table 4.6 lists the LST distribution statuses during the duration of the investigation.

Table 4. 4. Trends in the land surface temperature distribution from 1987 to 2023 in Asella and the surrounding area.

Area coverage during study period (km^2)			
	1987	**2005**	**2023**
<19	122.7087	93.8358	0.0522
19-22	111.3192	95.5926	60.2244
22-27	197.8425	165.9978	31.3227
27-31	392.8705	416.9925	66.4505
31-35	135.5688	184.8744	160.5627
>35	0.6048	3.7314	642.402

There has been a noticeable increase in LST in Asella and its surrounding areas over time, as indicated by the expanding coverage area in square kilometers. Figure 4.11 provides a detailed comparison of LST distributions for the selected years. This figure not only illustrates the distribution of LST across different regions but also highlights the consistent annual rise in temperature observed throughout the study period. The data presented in the figure demonstrates the ongoing upward trend in LST, indicating significant changes in the thermal landscape of the study regions.

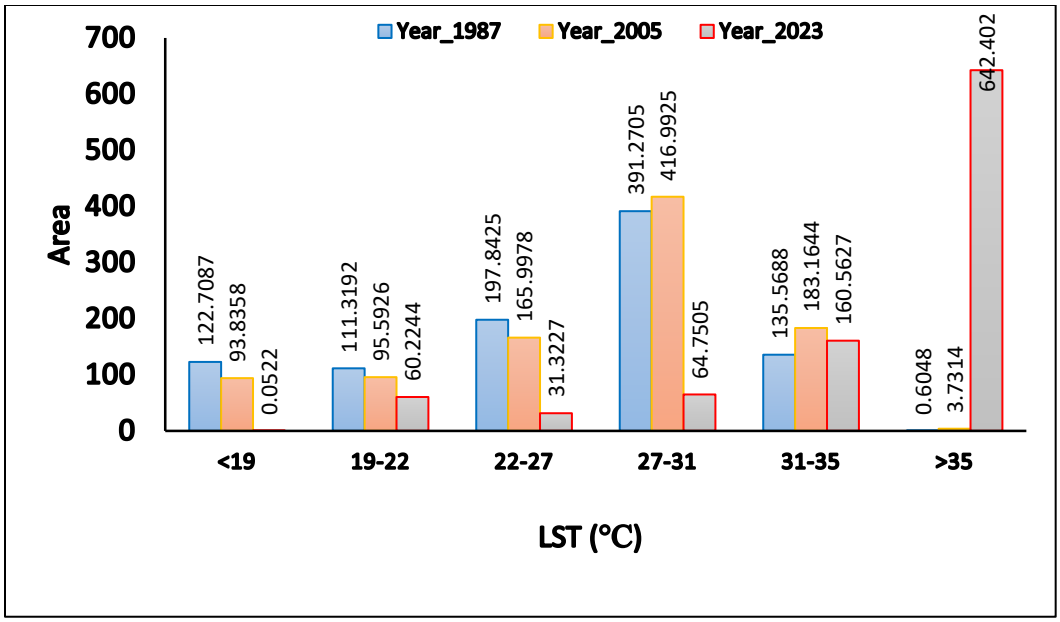

Figure 4. 10. Comparisons between LST distributions of the years 1987, 2005, and 2023 in the study area

4.12. Verification of the result for land surface temperature

There is a direct correlation between the interpolated atmospheric temperature and the LST obtained from the Landsat thermal band in the research region. However, it is important to note that the Landsat imagery used in this study was captured during dry weather and the harvesting season, which influenced the determined LST trend. To validate the spatial distribution of the Landsat imagery, the account was taken of the current meteorological conditions and the time at which the Landsat data was acquired. To confirm the land surface temperature, LU/LC classes and meteorological data from the research area were considered, along with GPS data collected from the field and Google Earth. Meteorological data from the five stations in the research area were used to interpolate temperature and rainfall.

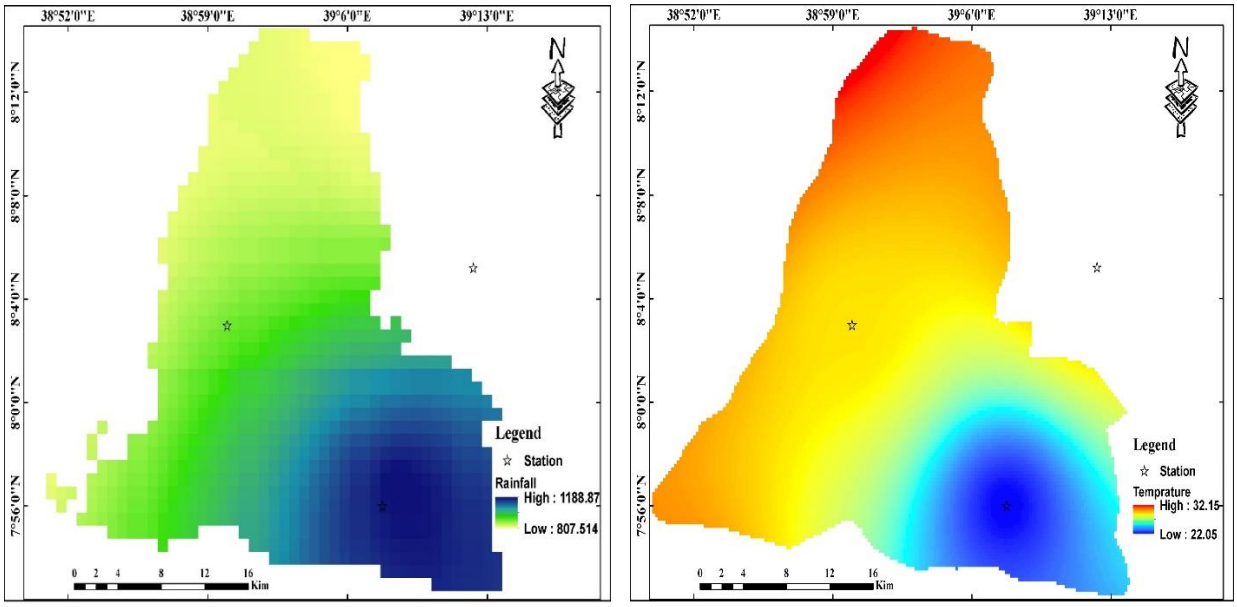

a) Rainfall map (mm) b) b) A temperature map in (ºC)

Figure 4. 11. A rainfall and a temperature-interpolated map of the research area

The interpolated map of the research region reveals that the central part of the area experienced average rainfall and temperature. However, the temperature maps of the northern, northwest, and northeastern regions indicate higher values compared to the southern regions. In particular, the northeast region registered a temperature value of 32.15 ºC, as reported by the interpolated map. On the other hand, the rainfall map demonstrates that the southeast and south areas experienced higher rainfall values than the northern regions. The findings of the Landsat thermal band LST extraction also revealed that the northern region consistently experienced the highest temperature values during the research periods, whereas the southeast and southwest regions had relatively lower values. However, it is worth noting that LST was particularly low in the Chillalo Terara region, which is densely covered in forest. For instance, in the Ziway water bodies, the LST was significantly lower. However, due to the interpolation assumption, the interpolated map depicts a more moderate temperature. The mean LST values obtained during the study period ranged from 19 ºC to 35 ºC. In contrast, the resulting interpolated atmospheric temperatures varied between 22.05 ºC and 32.15 ºC.

CHAPTER FIVE

DISCUSSION

5.1. Land-use/land-cover status of Asella and its surrounding area

The LU/LC changes observed in Asella and its surrounding areas are a result of population growth and the increasing demand for land for settlements and agriculture. These changes have hurt the environment. According to Houghton (1994), the main factors contributing to LU/LC variability are human population growth, economic development, technology, and environmental changes. The present study confirms that significant alterations in LU/LC occurred during the study period. In 1987, the area dedicated to settlements was 47.72 km², which increased to 80.58 km² in 2023. This is clear evidence of the growing need for settlement areas. Between 1987 and 2023, there was a significant increase in farmland within the study area. Initially, in 1987, the farmland covered an area of 512.24 km². Over time, this area steadily expanded to 560.36 km² by 2005. By 2023, the farmland had further increased to 653.26 km², demonstrating substantial agricultural development over the years. In contrast, the area of shrubland experienced a dramatic decline over the same period. In 1987, the shrubland covered 165.06 km², but by 2023, it had decreased significantly to 53.94 km². Similarly, the area of bare land also saw a reduction, decreasing from 112.46 km² in 1987 to 43.31 km² in 2023. These changes indicate significant transformations in LU/LC within the study area throughout the past few decades. The forest cover showed fluctuations. In summary, the classified satellite images provide evidence of changes in LU/LC.

5.2. Normalized difference vegetation index

The normalized disparity LST is calculated using the vegetation index, which provides an estimation of vegetation condition. According to Mihai (2012) and Weng (2004), the NDVI is a reliable indicator of both dryness and LST. The study's findings indicate that the NDVI varies across the study area, ranging from southeast and southwest to northeast and northwest. This variability in NDVI is in line with the varying vegetation cover in the predominantly farming-dominated study area. In evaluating the relationship between LST and NDVI for 2023, this study obtained an R^2 value of 0.95.57, indicating that 95.57% of the distribution of LST can be explained by NDVI, thereby highlighting the influence of vegetation state on LST. Consequently, this study observed a strong correlation between NDVI and LST, excluding the water body class.

5.3. Land surface temperature

Quantifying the area's LST required careful consideration of the thermal band in the Landsat image. In the current study, farmland, settlement, and bare land exhibited higher LST values. The primary reason for these high LST values and lower NDVI in the rural LU/LC class is that the image was taken during the dry season in November, December, and January. These months coincide with the main harvesting period in Ethiopia. Consequently, the agricultural, barren ground and settlement areas had high surface reflectance due to the dryness of the land post-crop harvest. As a result, water bodies, barren ground, settlements, and agricultural areas had lower NDVI values. However, shrubland and forest areas showed relatively higher NDVI values. Determining the relationship between LU/LC types and satellite-based thermal assessment of LST is crucial. The NDVI plays an important role in evaluating and researching LST. There are indirect correlations between LST and NDVI in various LU/LC categories, except for aquatic bodies. The NDVI value of vegetation and the type of LU/LC influence the LST value. However, it is important to note that the type of LU/LC is not the sole factor contributing to changes in LST. The LST value can increase or decrease depending on other circumstances, such as soil types, climate, elevation, geological context, and geothermal energy in the region.

Many researchers utilized thermal bands to investigate LST. Gebrekidan Worku (2016) examined Addis Ababa's LST status using Landsat satellite images. The link between LU/LC, LST, and NDVI was examined in the study. The NDVI and LST values were discovered to be negatively correlated by Gebrekidan Worku (2016). Because of the water body's low NDVI and LST values, it should be regarded as an exception in this instance. The current study's findings demonstrate that, during the investigation period, various LU/LC had varying NDVI and LST values.

There is an indirect, negative association between the LST and the normalized differential vegetation index. That might, however, be a direct and beneficial interaction, particularly in places where bodies of water and geothermal activity have a large potential. Negative values are indicative of non-reflecting surfaces like clouds, water, snow, and other non-vegetated locations, whereas positive values are reflective surfaces like vegetated areas., according to Burgan, and Bartlette, (1993). That does not imply, however, that all NDVI negative values have high LST values. The earth's surface's ability to reflect heat determines the land surface temperature. Regions

without vegetation and surfaces that are not reflecting typically have higher LST than regions with vegetation and bodies of water.

The findings of the study reveal six main LU/LC classes, each with different LST values. The LST of bare land, farms, and settlements is higher than that of water bodies, forests, and shrublands. The spatial and temporal distribution of LST in 1987, 2005, and 2023 demonstrates significant changes in the region over the research period. In 1987, the distribution of LST ranged from 8.74ºC to 37.55ºC. In contrast, the range for the lowest and highest LST in 2005 and 2023 was 9.90ºC to 40.46ºC and 18.59ºC to 48.85ºC, respectively. Therefore, LST exhibited a rising trend in response to changes in LU/LC and other factors.

Building upon the relationship previously discussed between LST and LU/LC types, it is important to also take into account other factors that affect LST variability. In addition to vegetation cover and seasonal changes, factors such as local soil types, altitude, geological context, and even geothermal influences all contribute to the patterns observed in LST. For example, areas with higher geothermal activity or specific geological formations may have higher LST values, even if they are covered by vegetation. Having a clear understanding of these localized factors is crucial for accurately assessing LST and for comprehensively interpreting the thermal dynamics of different landscapes.

CHAPTER SIX

CONCLUSION AND RECOMMENDATIONS

6.1. Conclusion

Geospatial tools are incredibly advantageous and play a pivotal role in helping researchers analyze trends in land use/land cover and land surface temperature. They are crucial in identifying vulnerable areas, understanding the contributing factors, and developing strategies to mitigate these issues. In terms of time, simplicity, and cost, these tools are the most efficient and effective option available. Applications such as environmental management initiatives and LU/LC change monitoring greatly benefit from the use of satellite data. Landsat imagery can be utilized to investigate the spatial distribution of LST and the dynamics of LU/LC. In this study, LU/LC was evaluated and its relationship to LST was examined using Landsat TM 5, ETM+7, and Landsat OLI/TIRS images. The calculated LST and LU/LC data obtained from these images provide crucial information for tracking environmental and human activity changes. Landsat data was particularly helpful in mapping LU/LC change, NDVI, and LST in Asella and its surrounding areas. The LU/LC pattern in the study area is influenced by socioeconomic and environmental factors, which are temporally and spatially exploited. Water bodies and vegetation classes (such as forests and shrublands) exhibited the lowest LST values, while settlements, bare ground, and farming areas had the highest LST values. The LU/LC in the region has undergone periodic changes, which have impacted LST. Over the years, the lowest and maximum LST values have consistently increased. Consequently, the calculated LST affects local temperatures and plays a significant role in LU/LC functions.

The study's conclusions showed that there was an increase in LSTs in 1987, 2005, and 2023. This increase was due to variations in the local climate, human activity, and LU/LC fluctuations. The study found a significant difference in LST between different LU/LC types in the study area. It was also observed that the LST values obtained from satellite data and the estimated temperature values from the weather stations used in the study were in good agreement. Furthermore, the computed NDVI values from satellite data were found to be a reliable indicator of the LST conditions in the research area. Therefore, the use of Geographic Information Systems (GIS) and

remote sensing data to analyze changes in LST and LU/LC patterns in the research area offers a faster and more cost-effective method that can cover a large area.

4.2. Recommendations

In the study's findings, which used Landsat imagery from 1987 and 2023, the main focus was on LU/CC and its relationship to LST in Asella and its surrounding areas. The study found that the LST value varies across different LU/LC classes and that there is potential for converting one type of LU/CC to another, such as farmland to settlement or vegetation area to farmland. However, it should be noted that there are situations where such modifications could positively impact LST. For instance, the planting of eucalyptus trees and certain perennial crops was found to result in a lower LST value. Based on these findings, the following recommendations are proposed.

- Develop comprehensive plans and policies for land use that incorporate economic, social, and environmental considerations, with a focus on promoting sustainable practices. Additionally, ensure that these plans are efficiently implemented and regularly reviewed and updated.

- The use of geospatial tools is highly beneficial and plays a crucial role for environmental researchers. These tools enable them to analyze land cover patterns and LST, identify vulnerable areas, comprehend their causes, and develop strategies. Geospatial tools are not only efficient and effective, but they also save time, simplify processes, and reduce costs..

- Promoting the planting of native and climate-adaptive tree species and increasing conservation efforts through the expansion of urban and rural green spaces, particularly in densely populated and barren areas.

- Establish an effective framework for overseeing and controlling LU/CC, and engage nearby communities in sustainable land management practices by providing them with resources and knowledge.

References.

Ali. (2009). Land use and land cover change, drivers and its impact: A comparative study from Kuhar Michael and Lenche Dima of the Blue Nile and Awash Basins of Ethiopia. *Cgspace.Cgiar.Org*, *August*.

Agarwal, C., Green, G. M., Grove, J. M., Evans, T. P., and Schweik, C. M. (2002). A review and assessment of land-use change models: dynamics of space, time, and human choice.

Attri, P., Chaudhry, S., & Sharma, S. (2015). *Remote Sensing & GIS-based Approaches for LULC Change Detection – A Remote Sensing & GIS-based Approaches for LULC Change Detection – A Review*. *May 2018*.

Ayanlade, A., Aigbiremolen, M. I., & Oladosu, O. R. (2021). Variations in urban land surface temperature intensity over four cities in different ecological zones. *Scientific Reports*, 1–17. https://doi.org/10.1038/s41598-021-99693-z

Balew, A., & Korme, T. (2020). The Egyptian Journal of Remote Sensing and Space Sciences Monitoring land surface temperature in Bahir Dar city and its surroundings using Landsat images. *The Egyptian Journal of Remote Sensing and Space Sciences*, *23*(3), 371–386. https://doi.org/10.1016/j.ejrs.2020.02.001

Basin, S. H. (2020). *Controls of Climate and Land-Use Change on Terrestrial Net Primary Productivity Variation in a Subtropical Humid Basin*.

Briassoulis, H. (2009). *Factors influencing land-use and land-cover change. Land cover, land use, and the global change, encyclopedia of life support systems*. *I*, 126–146.

Briassoulis, H. (2020). *The Web Book of Regional Science Sponsored by Analysis of Land Use Change : Theoretical and Modeling Approaches By Helen Briassoulis Department of Geography*.

Chaithanya et al. (2017). *Estimation of the Relationship between Urban Vegetation and Land Surface Temperature of Calicut City and Suburbs, Kerala, India using GIS and Remote Sensing data Estimation of the Relationship between Urban Vegetation and Land Surface*

Temperature of Cal. *October*. https://doi.org/10.23953/cloud.ijarsg.112

Coppin, P. R., and Bauer, M. E. (1996). Digital change detection in forest ecosystems with remote sensing imagery. Remote sensing reviews, 13(3-4), 207–234.

Coll, C., Caselles, V., Galve, J. M., Valor, E., Niclòs, R., & Sánchez, J. M. (2006). Evaluation of split-window and dual-angle correction methods for land surface temperature retrieval from Envisat/Advanced Along Track Scanning Radiometer (AATSR) data. Journal of Geophysical Research: Atmospheres, 111(D12).

Di Gregorio, A. (2005). Land cover classification system: classification concepts and user manual: LCCS (Vol. 2). Food & Agriculture Org.

Ellis, E. C. (2021). *Land Use and Ecological Change : A 12, 000-Year History*.

FAO/UNEP., (1999).Terminology for integrated resources planning and management. Food and agriculture organization/United Nations Environmental Program, Rome, Italy and Nairobi, Kenya.

Fasika, A., Motuma, T., & Gizaw, T. (2019). Land Use Land Cover Change Trend and Its Drivers in Somodo Watershed South Western, Ethiopia. *African Journal of Agricultural Research*, *14*(2), 102–117. https://doi.org/10.5897/ajar2018.13672

Friedl, M. A., Sulla-Menashe, D., Tan, B., Schneider, A., Ramankutty, N., Sibley, A., & Huang, X. (2010). MODIS Collection 5 global land cover: Algorithm refinements and characterization of new datasets. Remote sensing of Environment, 114(1), 168-182.

Gashaw, T., Bantider, A., & Mahari, A. (2014). *POPULATION DYNAMICS AND LAND USE / LAND COVER CHANGES IN DERA DISTRICT, ETHIOPIA*. *3*(1), 137–140.

Gemeda, D. O., Badasa, M., Dejene, I. N., & Deribew, K. T. (2023). *Impacts of forest cover change on carbon stock, carbon emission and land surface temperature in Sor watershed, Baro Akobo Basin, Western Ethiopia Impacts of forest cover change on carbon stock, carbon emission and land surface temperature in Sor water*. *August*. https://doi.org/10.2166/wcc.2023.208

Govind, N. R., & Ramesh, H. (2019). *The impact of spatiotemporal patterns of land use land cover and land surface temperature on an urban cool island : a case study of Bengaluru*.

Gowarda, S. N., Xueb, Y., & Czajkowskic, K. P. (2002). *Evaluating Land Surface Moisture Conditions From the Remotely Sensed Temperature / Vegetation Index Measurements – An Exploration With the Simplified Biosphere Model Evaluating land surface moisture conditions from the remotely sensed temperature / Vegeta*. *February*. https://doi.org/10.1016/S0034-4257(01)00275-9

Gries, T., Redlin, M., & Ugarte, J. E. (2019). *Human-induced climate change : the impact of land-use change*. 1031–1044.

Grimmond, S., The, S., & Journal, G. (2007). *Urbanization and global environmental change: local effects of urban warming*. *173*(1), 83–88.

Gupta, N., Mathew, A., & Khandelwal, S. (2020). Spatio-temporal impact assessment of land use/land cover (LU-LC) change on land surface temperatures over Jaipur city in India. *International Journal of Urban Sustainable Development*, *12*(3), 283–299. https://doi.org/10.1080/19463138.2020.1727908

Houghton, R. A. (1994). *The Worldwide Extent of Land-use Change*. *44*(5), 305–313.

Huang, S., Tang, L., Hupy, J. P., Wang, Y., & Shao, G. (2021). A commentary review on the use of normalized difference vegetation index (NDVI) in the era of popular remote sensing. *Journal of Forestry Research*, *32*(1), 1–6. https://doi.org/10.1007/s11676-020-01155-1

Ibitolu H.A. et al. (2017). Spatio-temporal analysis of land surface temperature variations in the rapidly developing Akure and its environs, southwestern Nigeria using Landsat data. *Ethiopian Journal of Environmental Studies and Management*, *10*(3), 389–403.

Imran, H. M., Hossain, A., Islam, A. K. M. S., Rahman, A., Bhuiyan, M. A. E., Paul, S., & Alam, A. (2021). Impact of Land Cover Changes on Land Surface Temperature and Human Thermal Comfort in Dhaka City of Bangladesh. *Earth Systems and Environment*, *5*(3), 667–693. https://doi.org/10.1007/s41748-021-00243-4

Jansen, L. J., & Di Gregorio, A. (2002). Parametric land cover and land-use classifications as tools for environmental change detection. *Food & Agriculture Org.*., *2*(manual), 89–100.

Javed, T., Li, Y., Feng, K., Ayantobo, O. O., Ahmad, S., Chen, X., Rashid, S., & Suon, S. (2021). *Monitoring responses of vegetation phenology and productivity to extreme climatic conditions using remote sensing across different sub-regions of China*. 3644–3659.

Joshi, S., Rai, N., Sharma, R., & Baral, N. (2021). Land use/land cover (LULC) change in suburb of Central Himalayas: a study from Chandragiri, Kathmandu. Journal of Forest and Environmental Science, 37(1), 44-51

Kafy, A. Al, Rahman, M. S., Faisal, A. Al, Hasan, M. M., & Islam, M. (2020). Modeling future land use land cover changes and their impacts on land surface temperatures in Rajshahi, Bangladesh. *Remote Sensing Applications: Society and Environment*, *18*(February), 100314. https://doi.org/10.1016/j.rsase.2020.100314

Kamusoko, C. (2022). Land Cover Classification Accuracy Assessment. *Springer Geography*, *80*, 105–118. https://doi.org/10.1007/978-981-16-5149-6_6

Kassouri, Y., & Adewole, O. (2022). *Land Use Policy Analysis of spatiotemporal Drivers and Convergence Characteristics of urban development in Africa*. *October*.

Kumar, P., & Gonencgil, B. (2023). *Effect on Land Surface Temperature in Lahaul and Spiti, India*. 1–20.

Lambin, E. F., & Meyfroidt, P. (2010). *Land Use Policy Land use transitions : Socio-ecological feedback versus socio-economic change*. *27*, 108–118. https://doi.org/10.1016/j.landusepol.2009.09.003

Li, Z., Tang, B., Wu, H., Ren, H., Yan, G., Wan, Z., Trigo, I. F., & Sobrino, J. A. (2013). Remote Sensing of Environment Satellite-derived land surface temperature : Current status and perspectives. *Remote Sensing of Environment*, *131*, 14–37. https://doi.org/10.1016/j.rse.2012.12.008

Maguire. (1991). An overview and definition of GIS. Geographical information systems:

Principles and applications, (pp. 1(1), 9–20).

Maitima, J. M., Mugatha, S. M., Reid, R. S., Gachimbi, L. N., Majule, A., Lyaruu, H., Pomery, D., Mathai, S., & Mugisha, S. (2009). *The linkages between land use change, land degradation, and biodiversity across East Africa*. *3*(10), 310–325.

Meyer, W. B., & Turner, B. L. (1992). *Human population growth and global land-use/cover change*.

Mihai,V.H.(2012).Using Satellite Images Landsat TM For calculating Normalized DifferenceIndexes for the landscape of Parang mountains.Lect.Ph.D.Eng.Banat University of Agricultural Sciences and Veterinary Medicine, Romania.

Miheretu Birhan and Assefa Abegaz (2017). Land use/land cover changes and their environmental implications in the Gelana sub-watershed of Northern highlands of Ethiopia. Environmental Systems Research, 6(1), 7.

Mirsanjari, M. M., Mohammadyari, F., Visockiene, J. S., & Zarandian, A. (2021). Relationship between land surface temperature and urbanization in Vilnius district. *Environmental Monitoring and Assessment*, 1–14. https://doi.org/10.1007/s10661-021-09209-5

Mo, Y., Xu, Y., Chen, H., & Zhu, S. (2021). *A Review of Reconstructing Remotely Sensed Land Surface Temperature under Cloudy Conditions*.

Mohanrajan, S. N., & Loganathan, A. (2020). *Survey on Land Use / Land Cover (LU / LC) change analysis in remote sensing and GIS environment : Techniques and Challenges*. 29900–29926.

Odindi. (2015). *Assessing the Value of Urban Green Spaces in Mitigating Multi-Seasonal Urban Heat using MODIS Land Surface Temperature (LST) and Landsat 8 data*. *9*(1), 9–18.

Oluseyi. (2011). *Managing Land Use Transformation and Land Surface Temperature Change in Anyigba Town, Kogi State, Nigeria*. *3*(1), 77–85. https://doi.org/10.5539/jgg.v3n1p77

Omeno, M. O., Yu, Y., Fan, W., Lubalega, T., Chen, C., Kachaka, C., & Kaiko, S. (2021). *Analysis*

of the Impact of Land-Use / Land-Cover Change on Land-Surface Temperature in the Villages within the Luki Biosphere Reserve.

Prata, A. J., V. Casellescoll, C., Sobrino, J. A., & Ottle, C. (1995). Thermal remote sensing of land surface temperature from satellites: current status and prospects. *Remote Sensing Reviews*, *12*(3–4), 175–224. https://doi.org/10.1080/02757259509532285

Rajeshwari, A., & Mani, N. D. (2014). *ESTIMATION OF LAND SURFACE TEMPERATURE OF DINDIGUL DISTRICT USING LANDSAT 8 DATA*. 122–126.

Ramachandra, T. V. (2021). *Land Surface Temperature Analysis in an Urbanising Landscape through Multi-Resolution data Land Surface Temperature Analysis in an Urbanising Landscape through Multi-Resolution Data Centre for infrastructure, Sustainable Transportation and Urban Planning*. *June 2012*.

Ramankutty, N., Graumlich, L., Achard, F., Alves, D., Chhabra, A., DeFries, R. S., ... & Turner, B. L. (2006). Global Land-Cover Change: Recent Progress, Remaining Challenges. *Springer, Global land-cover change: Recent progress, remaining challenges*, 9–39.

Reddy, G. O. (2018). Geospatial Technologies in Land Resources Mapping, Monitoring and Management. *Springer*, 45-62.

Reid, R. S., Kruska, R. L., Muthui, N., Taye, A., Wotton, S., Wilson, C. J., & Mulatu, W. (2000). *Land-use and land-cover dynamics in response to changes in climatic, biological and socio-political forces : the case of southwestern Ethiopia*. *Penner 1994*, 339–355.

Seyam, M. M. H., Haque, M. R., & Rahman, M. M. (2023). Identifying the land use land cover (LULC) changes using remote sensing and GIS approach: A case study at Bhaluka in Mymensingh, Bangladesh. *Case Studies in Chemical and Environmental Engineering*, *7*(January), 100293. https://doi.org/10.1016/j.cscee.2022.100293

Shukla, A. J., Nobre, C., & Sellers, P. (1990). Amazon Deforestation and Climate Change Published by : American Association for the Advancement of Science Stable URL : https://www.jstor.org/stable/2873721 American Association for the Advancement of Science is collaborating with JSTOR to digitize, pres. 247(4948), 1322–1325.

Singh, R. B., Grover, A., & Zhan, J. (2014). Inter-Seasonal Variations of Surface Temperature in the Urbanized Environment of Delhi Using Landsat Thermal Data. 1811–1828. https://doi.org/10.3390/en7031811

Smith, P. (2014). Agriculture, Forestry and Other Land Use (AFOLU).

Sobrino, J. A., Oltra-carrió, R., Sòria, G., & Jiménez-muñoz, J. C. (2012). Evaluation of the surface urban heat island effect in the city of Madrid by thermal remote sensing. 34, 3177–3192.

Solaimani, K., Sciences, S. A., Arekhi, M., & Tamartash, R. R. (2010). Land use/cover change detection based on remote sensing data (A case study ; Neka Basin) Land use/cover change detection based on remote sensing data (A case study ; Neka Basin) M . Sc student of Range Management, University of Agriculture and Na. November. https://doi.org/10.5251/abjna.2010.1.6.1148.1157

Sresto, M. A., Siddika, S., Fattah, A., Morshed, S. R., & Morshed, M. (2022). Heliyon A GIS and remote sensing approach for measuring summer-winter variation of land use and land cover indices and surface temperature in Dhaka district, Bangladesh. *Heliyon*, *8*(February), e10309. https://doi.org/10.1016/j.heliyon.2022.e10309

Sruthi, S., & Aslam, M. A. M. (2015). INTERNATIONAL CONFERENCE ON WATER RESOURCES, COASTAL AND OCEAN ENGINEERING (ICWRCOE 2015) Agricultural Drought Analysis Using the NDVI and Land Surface Temperature Data ; a Case Study of Raichur District. *Aquatic Procedia*, *4*(Icwrcoe), 1258–1264. https://doi.org/10.1016/j.aqpro.2015.02.164

Sun, J., & He, J. (2009). *Influence of Land Use and Land Cover Change on Land Surface Temperature*. *01038*, 1–7.

Tafesse, B., & Suryabhagavan, K. V. (2019). Systematic modeling of impacts of land-use and land-cover changes on land surface temperature in Adama Zuria District, Ethiopia. *Modeling Earth Systems and Environment*, *5*(3), 805–817. https://doi.org/10.1007/s40808-018-0567-1

Thapa, P. S., Awasthi, K. D., Regmi, R. R., & Oli, B. N. (2022). *An Assessment of Forest Cover and Land Use Changes in Laljhadi Corridor Using GIS and Remote Sensing An Assessment*

of Forest Cover and Land Use Changes in Laljhadi Corridor Using GIS and Remote Sensing. *June*.

Thornton, P., & Herrero, M. (2010). *The Inter-linkages between Rapid Growth in Livestock Production, Climate Change, and the Impacts on Water Resources, Land Use, and Deforestation*. *January*.

Trigo, I. F., Monteiro, I. T., Olesen, F., & Kabsch, E. (2008). *An assessment of remotely sensed land surface temperature*. *113*(June), 1–12. https://doi.org/10.1029/2008JD010035

Walther, B. A., & Moore, J. L. (2005). *The Concepts of Bias, Precision, and Accuracy, and Their Use in Testing the Performance of Species Richness Estimators, with a Literature Review of Estimator Performance Author (s): Bruno A . Walther, Joslin L . Moore and Carsten Rahbek Published by*. *28*(6), 815–829.

Wheeler, T., & Von Braun, J. (2013). Climate change impacts on global food security. *Science*, *341*(6145), 508–513. https://doi.org/10.1126/science.1239402

Wulder, M. A., Coops, N. C., Roy, D. P., White, J. C., Wulder, M. A., Coops, N. C., Roy, D. P., White, J. C., Wulder, M. A., Coops, N. C., Roy, D. P., & White, J. C. (2018). Land cover 2.0. *International Journal of Remote Sensing*, *39*(12), 4254–4284. https://doi.org/10.1080/01431161.2018.1452075

Zhang, J., Jiao, G., & Ye, Q. (2022). *The Impact of Urban Expansion on the Urban Thermal Environment : A Case Study in Nanchang, Jiangxi, China*.

Zubair. (2006). Change detection in land use and Land cover using remote sensing data and GIS (A case study of Ilorin and its environs in Kwara State). *Indonesian Journal of Forestry Research*, *7*, 176.

Appendices

Appendices 1: Classification accuracy assessment report for the year 1987.

Class	Forest	Shrub land	Farmland	Settlement	Waterbody	Bare land	Total	U_Accuracy	Kappa
Forest	18	2	4	0	0	0	24	0.75	0
Shrub land	2	28	11	0	0	0	41	0.682927	0
Farmland	1	3	149	0	0	3	156	0.955128	0
Settlement	0	2	5	10	0	4	21	0.7619	0
Waterbody	0	0	1	0	15	0	16	0.9375	0
Bare land	0	0	4	1	0	37	42	0.880952	0
Total	21	35	174	11	15	44	300	0	0
P_Accuracy	0.8571	0.8	0.856322	0.909091	1	0.840909	0	**0.856667**	0
Kappa	0	0	0	0	0	0	0	0	**0.8086**

Appendices 2**:** Classification accuracy assessment report for the year 2005.

Class	Forest	Shrub land	Farmland	Settlement	Waterbody	Bare land	Total	U_Accuracy	Kappa
Forest	26	3	2	0	0	2	33	0.787879	0
Shrub land	1	26	1	0	0	1	29	0.896552	0
Farmland	0	8	151	0	1	8	168	0.89881	0
Settlement	0	1	3	12	0	4	20	0.6	0
Waterbody	0	0	0	0	19	0	19	1	0
Bare land	0	0	3	0	0	28	31	0.903226	0
Total	27	38	160	12	20	43	300	0	0
P_Accuracy	0.963	0.684211	0.94375	1	0.95	0.651163	0	**0.873333**	0
Kappa	0	0	0	0	0	0	0	0	**0.8073**

Appendices 3: Classification accuracy assessment report for the year 2023

Class	Forest	Shrub land	Farmland	Settlement	Waterbody	Bare land	Total	U_Accuracy	Kappa
Forest	19	0	0	0	0	0	19	1	0
Shrub land	2	10	2	0	0	0	14	0.714286	0
Farmland	1	5	156	0	0	5	167	0.934132	0
Settlement	2	1	2	15	0	2	22	0.681818	0
Waterbody	0	0	0	0	15	0	15	1	0
Bare land	0	0	3	0	0	9	12	0.75	0
Total	24	16	163	15	15	16	249	0	0
P_Accuracy	0.7917	0.625	0.957055	1	1	0.5625	0	**0.899598**	0
Kappa	0	0	0	0	0	0	0	0	**0.8134**

Appendices 4**.** Plate 1: A variety of LU/LC photo samples.

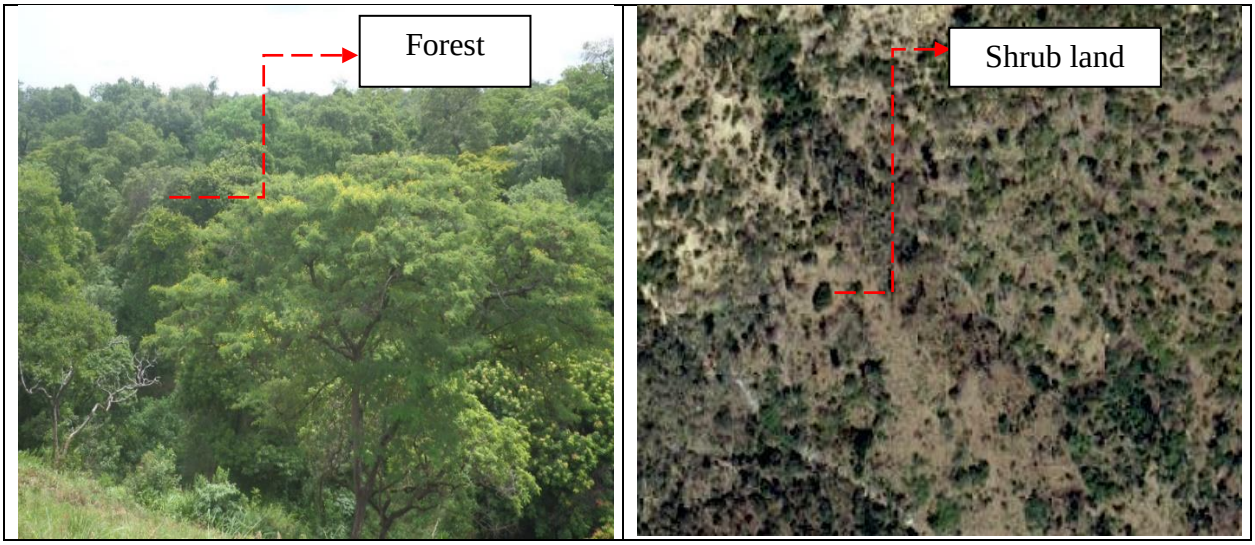


Farmland
Settlement
Waterbody
Bare land

Appendices 5. Map 1: GPS point data map.

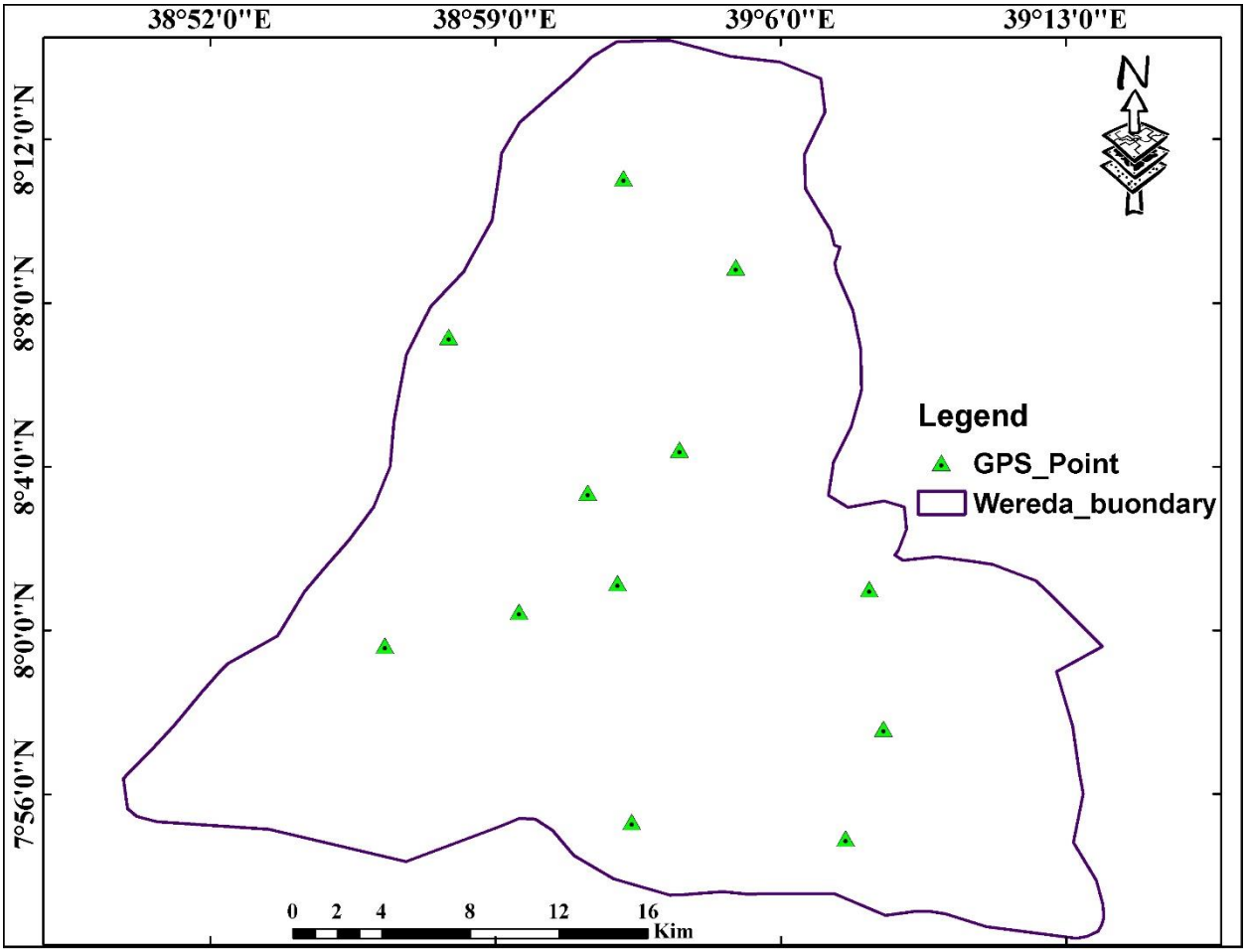

Appendices 6. Map 2: Showing of weather stations.

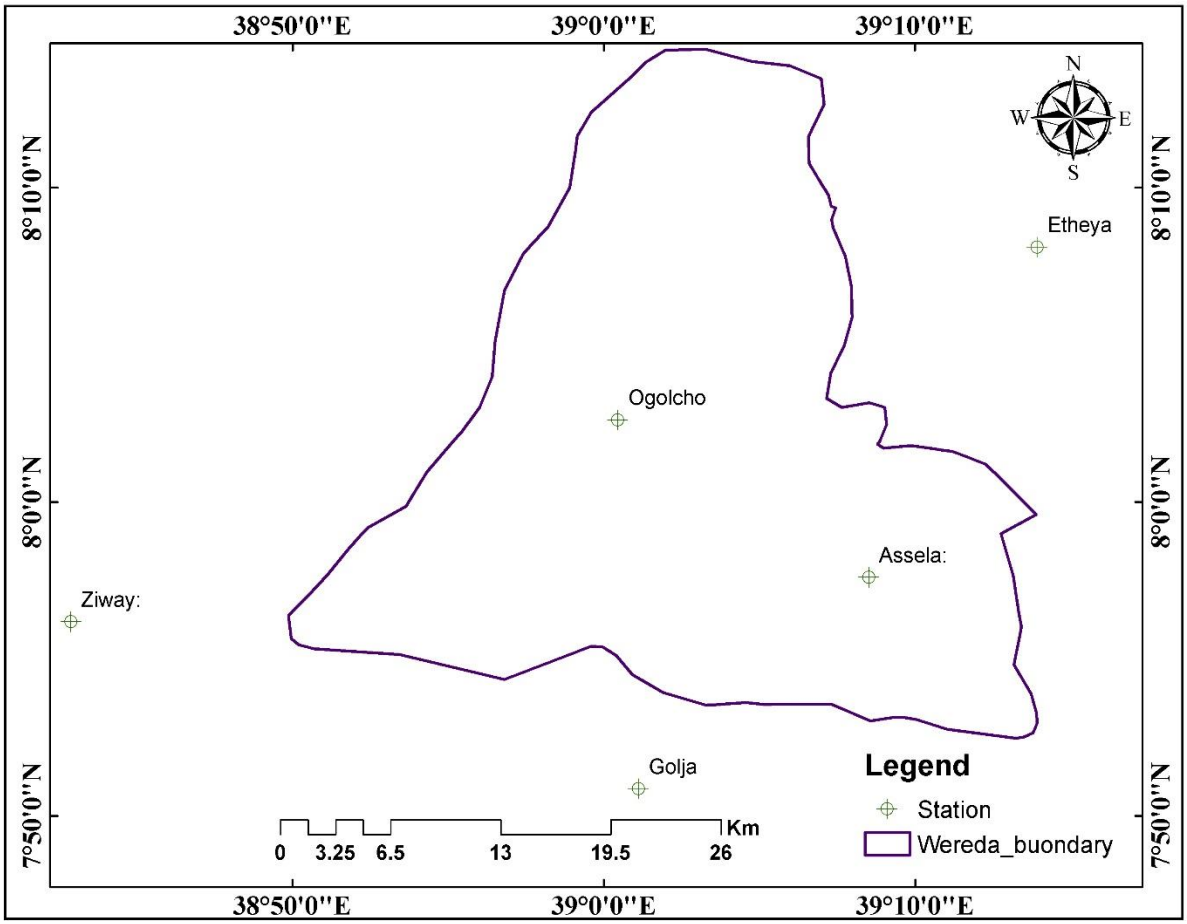

DECLARATION

I, the undersigned, hereby certify that my work is included in the thesis. As per the globally recognized standards, I have credited and referenced all sources utilized in this project.

I am aware that failing to uphold the standards of academic honesty and integrity, as well as misrepresenting or fabricating any ideas, data, facts, or sources, will be sufficient justification for punitive action from the sources that have not been correctly referenced or recognized, as well as disciplinary action by the university.

Name: Dawit Desalegn Tola

Signature: _____

Date: _____